J Physiol 597.3 (2019) pp 679–698

The Journal of Physiology

TOPICAL REVIEW

Challenges and advances in atomistic simulations of potassium and sodium ion channel gating and permeation

Kevin R. DeMarco[1,2], Slava Bekker[1,3] and Igor Vorobyov[1,2]

[1] *Department of Physiology and Membrane Biology, School of Medicine, University of California, Davis, CA, USA*
[2] *Department of Pharmacology, School of Medicine, University of California, Davis, CA, USA*
[3] *Chemistry Department, American River College, Sacramento, CA, USA*

Edited by: Ole Petersen & Ruth Murrell-Lagnado

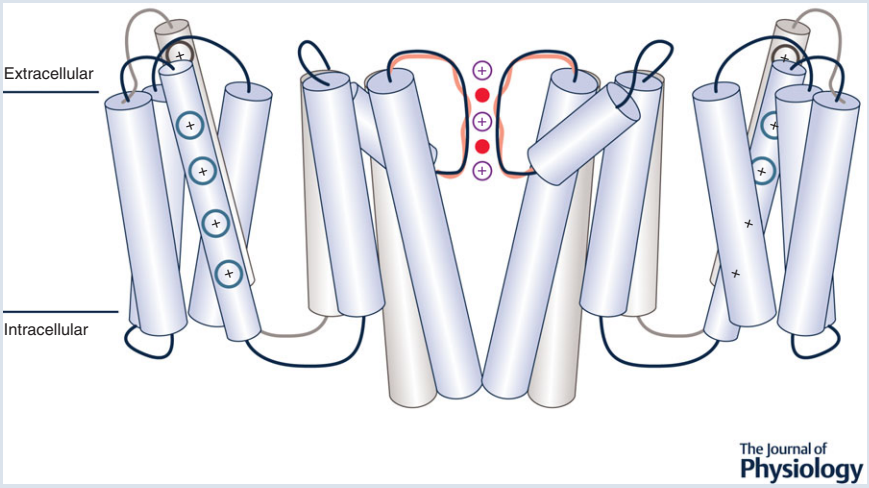

Abstract Ion channels are implicated in many essential physiological events such as electrical signal propagation and cellular communication. The advent of K^+ and Na^+ ion channel structure determination has facilitated numerous investigations of molecular determinants of their behaviour. At the same time, rapid development of computer hardware and molecular simulation methodologies has made computational studies of large biological molecules in all-atom representation tractable. The concurrent evolution of experimental structural biology with biomolecular computer modelling has yielded mechanistic details of fundamental processes unavailable through experiments alone, such as ion conduction and ion channel gating. This review is a short survey of the atomistic computational investigations of K^+ and Na^+ ion channels,

Kevin DeMarco obtained an MS in Physics from the University of Central Florida and PhD in Biophysics from the University of California, Davis, where he is currently a postdoctoral scholar. His academic interests range from quantum physics, to atomistic simulation of biomolecular systems, to applied multi-scale computational approaches in predictive pharmacology. **Slava Bekker** obtained a PhD in Chemistry in 2011 from the University of California, Davis, where she was a member of Toby Allen's lab. Her academic interests span computer simulations of proteins and cell membranes and chemistry education. She is currently a faculty member at American River College in Sacramento, CA and was a visiting scholar at the University of California, Davis in the summers of 2017 and 2018. **Igor Vorobyov** obtained a PhD in Chemistry in 2003 from the University of Louisville and worked in the research laboratories of Alex MacKerell, Toby Allen and Arieh Warshel. He is currently an assistant professor at the University of California, Davis, School of Medicine. His research interests focus on molecular modelling and simulations of membrane proteins, protein–lipid and drug interactions as well as development of new accurate computational models for their description.

DOI: 10.1113/JP277088

focusing on KcsA and several voltage-gated channels from the K_V and Na_V families, which have garnered many successes and engendered several long-standing controversies regarding the nature of their structure–function relationship. We review the latest advancements and challenges facing the field of molecular modelling and simulation regarding the structural and energetic determinants of ion channel function and their agreement with experimental observations.

(Resubmitted 22 September 2018; accepted after revision 15 October 2018; first published online 24 November 2018)
Corresponding author I. Vorobyov: Department of Physiology and Membrane Biology, University of California, Davis, 4303 Tupper Hall, One Shields Ave, Davis, CA 95616–8636, USA. Email: ivorobyov@ucdavis.edu

Abstract figure legend Structural illustration of the voltage-gated potassium channel gating transitions studied by atomistic molecular dynamics simulations including voltage-dependent activation/deactivation associated with channel pore opening and closing and voltage sensor domain (VSD) movement as well as C-type inactivation processes associated with selectivity filter distortions. A single file of alternating K^+ ions and water molecules in the selectivity filter demonstrates a starting configuration for a knock-on conduction mechanism. Resting VSD/closed pore structure is shown using light-blue contours, and activated VSD/open pore is shown using grey contours. α-Helices are shown by white cylinders and loops by black/grey curves. Distorted (inactivated) selectivity filter (SF) is shown in pink. Charged residues on S4 are shown by blue/gray circles, K^+ ions and water molecules in the SF are shown in purple and red, respectively. Illustrations are based on EAG (Whicher & MacKinnon, 2016) and hERG (Wang & MacKinnon, 2017) cryo-EM structures.

Introduction

Ion channels are a diverse group of membrane transport proteins, with nearly 300 so far identified in the human genome (Southan *et al.* 2016). They are critical facilitators of the passive translocation of ions across cell membranes, since the hydrophobic nature of biomembranes surrounding cells and subcellular organelles makes them highly impermeable to charged species (Gennis, 1989). Ion channels are present in single-cell organisms as well as in the majority of cell types of multicellular organisms (Hille *et al.* 1999), where they perform diverse functions such as biosensing, signalling and maintaining homeostasis. In electrically excitable cells such as neurons and cardiac myocytes, ion channels are responsible for the extremely rapid propagation of electrical signals driven by the generation of action potentials (Hille, 2001). Ion channels represent important drug targets (Overington *et al.* 2006), but there have been substantial challenges with therapeutic applications that are both sensitive and selective to specific ion channel subtypes. Moreover, some ion channels, such as K_V11.1, encoded by the human *ether-à-go-go*-related gene (hERG), are major drug anti-targets since certain ion channel–drug interactions may cause deadly arrhythmias and other cardiac disorders (Vandenberg *et al.* 2012), often leading to the withdrawal of a prospective drug from the market (Colatsky *et al.* 2016). In addition, ion channel mutations may lead to various neurological, cardiac, muscular, systemic and other serious health disorders called channelopathies (Kass, 2005). Therefore, a molecular-level understanding of ion channel physiology is of the utmost biomedical significance.

Publication of the first atomic-resolution crystal structure of a bacterial K^+ selective KcsA channel in 1998 (Doyle *et al.* 1998) brought about a breakthrough in understanding of ion channel molecular architecture, necessary for structural modelling studies. The structures of several voltage-gated K^+ (K_V) and Na^+ (Na_V) channels followed (illustrated in Fig. 1 for K_V11.1), and revealed a common homotetrameric pore domain (PD), with each monomer comprising two transmembrane (TM) α-helices (aqueous pore-lining inner S6 and lipid-facing outer S5) linked through extracellular loops and short pore helices, and the narrowest constriction of the pore forming a selectivity filter (SF) (Doyle *et al.* 1998; Jiang *et al.* 2003; Payandeh *et al.* 2011). For channels in the K_V and Na_V families, flexible linkers connect the PDs to voltage sensing domains (VSD), which typically consist of four TM helices (S1–S4) per monomer (see Fig. 1) and move in response to a change in TM electrical potential, thereby exerting a mechanical effect on the PD, leading to channel opening or closing (Jiang *et al.* 2003; Payandeh *et al.* 2011).

How molecular modelling and simulation methodology can complement experiment

Currently, there are several dozen structures of ion channels from different organisms and protein families in the Protein Data Bank (PDB). Most of them are bacterial and were obtained by high resolution by X-ray crystallography, but in the past few years a resolution revolution in cryogenic electron microscopy (cryo-EM) has led to the determination of many eukaryotic ion channel structures, but at lower resolution (e.g. 3–4 Å) than is possible with X-ray structures (Shen *et al.* 2017; Wang & MacKinnon, 2017). In addition to resolution, one major concern with protein structures obtained

from either X-ray crystallography or cryo-EM is whether they are representative of the structures at physiological conditions. There is the potential for ion channel protein structures to undergo substantial modifications from physiological conditions due to the incorporation of buffer solutions, detergents, crystal packing and heavy atom staining (in X-ray), and vitreous ice and radiation damage (in cryo-EM) (Ubarretxena-Belandia & Stokes, 2010; Palamini *et al.* 2016; Rawson *et al.* 2016). Along with the extremely low temperatures used for structural determination, all of these factors have the potential to induce artificial protein conformations, although the close similarity between X-ray detergent and cryo-EM lipid nandodisc channel structures, such as that for K_V1.2/2.1 chimera (Matthies *et al.* 2018), is encouraging.

Molecular modelling can complement and overcome shortcomings of experimental techniques. Molecular modelling helps address some of the shortcomings of experimental structure determination by aiding in the refinement of low-resolution structures, and by the generation of models of channel isoforms, for which structures do not yet exist. While functional studies are largely consistent with experimentally resolved structures (Jiang *et al.* 2003; Lenaeus *et al.* 2017; Wang & MacKinnon, 2017), computer simulation and atomistic modelling are often the only techniques that can provide the necessary temporal and spatial resolution for evaluating structural stability. Furthermore, as the structures of many ion channels and other membrane proteins remain unresolved at this time, molecular homology modelling can serve as a powerful predictive tool that circumvents the challenges of *de novo* protein modelling (Koehler Leman *et al.* 2015). Homology modelling approaches assume that protein structure is more conserved than sequence. Such is usually the case for ion channels, where relatively low sequence similarities of 30–40% are accompanied by strong structural resemblance, deviating only by a few angstroms (Forrest *et al.* 2006). Multiple programs are available for generating homology models of protein structures, such as MODELLER (Fiser & Sali, 2003), Schrodinger Prime (Jacobson *et al.* 2004), HHPred (Zimmermann *et al.* 2018) and ROSETTA (Song *et al.* 2013). They use different algorithms for protein structure and energy predictions (Koehler Leman *et al.* 2015), but each has been successfully used for ion channel structural modelling in the past (Khalili-Araghi *et al.* 2010; Durdagi *et al.* 2012; Yarov-Yarovoy *et al.* 2012), and as of yet, no strong consensus exists for choosing the best program for this task.

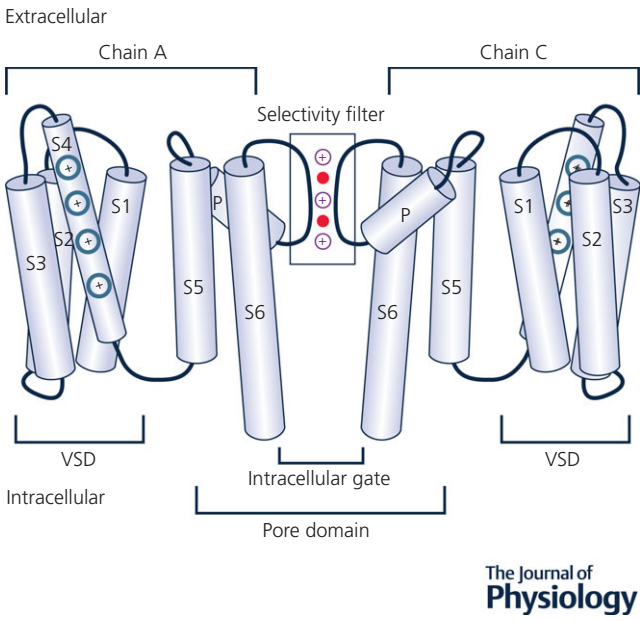

Figure 1. Topology of a K_V channel
The voltage-sensing domain (VSD), depicted in an activated conformation, is composed of transmembrane helices S1–S4 with charged residues on the S4 helix shown in blue. The pore domain is composed of transmembrane helices S5–S6, with an open intracellular gate near the bottom. α-Helices are shown by light-blue cylinders and loops by black curves. The selectivity filter (SF) region is shown by a rectangular box with three K^+ and coordinating water molecules in purple and red, respectively. Illustration is adapted from the published structure of hERG (Wang & MacKinnon, 2017), with two opposite chains (A and C) of the homotetramer shown.

Studying the motion of ion channels with molecular dynamics simulations. Insight into potentially important molecular interactions within a particular state of a protein structure can be gained from homology modelling; however, it cannot provide accurate thermodynamic and kinetic quantities of a simulated system. Molecular dynamics (MD) simulations, on the other hand, can be used to predict such data and thus serve as an invaluable tool to fully understand molecular mechanisms such as ion conduction and channel gating discussed in more detail below. MD is based on the numerical integration of Newton's equations of motion for a collection of particles, representing a molecular system of interest (Allen & Tildesley, 1987). In an all-atom representation of an ion channel, lipid membrane and solvent, a typical simulated system, illustrated in Fig. 2, totals around 10^5 atoms. The fastest molecular motions in a simulated system are the vibrational motions of bonds and angles, which occur on the order of femtoseconds (fs), thereby making it an upper bound for the time step used in MD numerical integration. Constraining the fastest vibrational motions (i.e. fixing atomic bond lengths and/or angles), as done in SHAKE (Ryckaert *et al.* 1977), SETTLE (Miyamoto & Kollman, 1992) and LINCS (Hess *et al.* 1997) algorithms, allows for an increased MD time step, and thus improved performance in those simulations. Also, multiple time steps for different types of interactions in molecular

systems can be used as implemented, for instance, in the RESPA method (Tuckerman *et al.* 1992).

Owing in part to the availability of faster and multiple-core processors, computer clusters with a large number of nodes with fast interconnects, graphical processor unit (GPU) computing, as well as efficient and highly scalable MD codes such as NAMD (Phillips *et al.* 2005), GROMACS (Hess *et al.* 2008), CHARMM (Brooks *et al.* 2009), OpenMM (Eastman *et al.* 2017), Desmond (Bowers *et al.* 2006), Tinker (Ponder, 2004) and Amber (Case *et al.* 2005), simulations of up to a few microseconds in duration are currently possible; a vast improvement over the nanosecond time scales that were possible just a few years ago. While simulations as long as few microseconds are often enough to study ion conduction, the time scale of channel gating is still out of reach. Nevertheless, the advent of special purpose supercomputers, such as Anton 2 by DE Shaw Research (Shaw *et al.* 2014), has facilitated multi-microsecond, and even millisecond, MD simulations, approaching the time scales of ion channel activation and deactivation. However, such long-time-scale MD simulations are still not feasible to run on most standard computer clusters. A timeline summarizing the physical and physiological time scales accessible with atomistic MD is shown in Fig. 3.

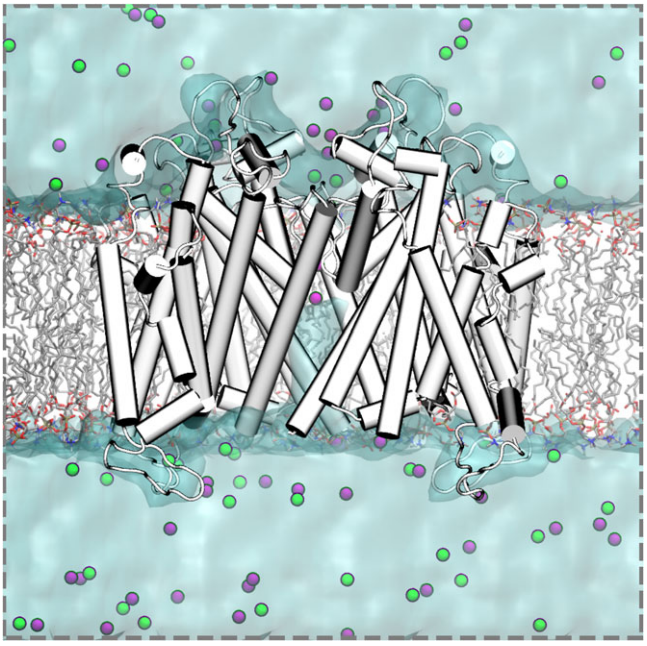

Figure 2. A typical ion channel all-atom MD simulation system consisting of hERG ion channel in hydrated lipid membrane
hERG ion channel with α-helices and loops depicted as white/gray cylinders and white curves, respectively, POPC (1-palmitoyl-2-oleoyl-*sn*-glycero-3-phosphocholine) lipid membrane in wireframe representation. C atoms, grey; O, red; N, blue; P, orange; H atoms are not shown; water is depicted as cyan molecular surface, and potassium and chloride ions are shown as purple and green balls, respectively.

Accessing long time scales with reduced system representations and enhanced sampling techniques. One alternative method to purpose-built supercomputers for achieving longer time-scale simulations is to reduce the number of atoms present in the system. For instance, the Grand Canonical Monte Carlo/Brownian Dynamics (GCMC/BD) is one such method, and has been used to study ion conduction (Im *et al.* 2000). In this reduced-system representation, water and lipid molecules are represented implicitly as a dielectric field, stationary protein atoms have fixed partial charges, while the ions are included explicitly. An even more reduced representation is one in which ionic density is modelled implicitly using a Boltzmann distribution, where the resultant electrostatic potential is obtained via numerical solutions to the linearized Poisson–Boltzmann (PB) equation, and ion transport is approximated with the Poisson–Nernst–Planck model (Maffeo *et al.* 2012). Furthermore, coarse-grained methodologies, in which a collection of atoms is represented as a single particle, have been used to study the large-scale motions related to ion channel gating (Treptow *et al.* 2008) and obtain corresponding free energy profiles (Kim & Warshel, 2014).

Another alternative approach to bridge relatively short simulation to much longer experimental time scales is to use enhanced sampling techniques, which allow a modelled system to cross large energetic barriers and sample regions of conformational space otherwise not amenable to brute-force application of unbiased MD methodology. This can be done in myriad ways, such as: (1) adding various restraints (umbrella sampling (Torrie & Valleau, 1977), adaptive biasing force (Darve *et al.* 2008) and metadynamics (Laio & Parrinello, 2002)), (2) application of additional forces or velocities to atoms moving in a set direction (steered (Isralewitz *et al.* 2001) or targeted MD (Schlitter *et al.* 1994)), (3) alchemical permutations of ions or amino acid residues (free energy perturbation; Kollman, 1993), or (4) so-called replica-exchange techniques that involve occasional system exchanges with a replica running at either increased temperature (Sugita & Okamoto, 1999) or with reduced interaction potentials (Fukunishi *et al.* 2002). All such techniques can be and have been applied to ion channel simulations (Roux *et al.* 2004; Maffeo *et al.* 2012), but the details extend beyond of scope of this review.

Atomistic force field accuracy and limitations. MD simulations are governed by empirical force field models, which describe atomic interactions in biomolecular systems using the laws of classical mechanics. Force fields are expressed as a potential energy function with empirically derived parameters for different chemical atom types (Mackerell, 2004), with the latter optimized to reproduce experimental and quantum-mechanical (QM) reference data for relevant system components, typically

emphasizing their properties in bulk aqueous solutions (Mackerell, 2004). For atomistic MD simulations of ion channels in explicitly hydrated lipid membranes (Fig. 2), empirical force fields for protein, lipids, water and ions are used. Examples of popular biomolecular force fields commonly used for such membrane protein simulations include CHARMM (Huang & MacKerell, 2013; Huang *et al.* 2017), Amber (Cornell *et al.* 1995), OPLS-AA (Kaminski *et al.* 2001) and GROMOS (Schmid *et al.* 2011).

In most protein force fields, the building blocks are individual amino acid residue models, which can be used to simulate any protein molecule, thus satisfying an important force field requirement: parameter transferability (Lopes *et al.* 2015). Force field parameters for both protein backbone and side chains are of crucial importance, and recent improvements have focused on reproducing backbone dihedral angle (ϕ, ψ) Ramachandran maps and side chain dihedral angles (Lopes *et al.* 2015) derived from QM calculations or experimental data. Lipid force fields are designed in a similar way, with the same parameters for functional groups (for instance, saturated hydrocarbon lipid tail, glycerol, and phosphodiester moieties) combined to obtain lipid molecule models aimed at reproducing several experimental properties for hydrated lipid assemblies, such as membrane thicknesses, areas per lipid, and deuterium order parameter profiles (Lyubartsev & Rabinovich, 2016). Typically, simple three-site (oxygen and two H atoms) rigid water models such as TIP3P (Jorgensen *et al.* 1983) and SPC/E (Berendsen *et al.* 1987), along with the aforementioned vibrational mode constraints (e.g. SHAKE or SETTLE), are used in combination for increased computational efficiency. However, more complex, and presumably more accurate, models such as TIP4P-Ew (Horn *et al.* 2004) are being increasingly utilized in biomolecular simulations (Onufriev & Izadi, 2018). Ion parameters are intimately tied to water models (Joung & Cheatham III, 2008), and all the force fields representing system components should be compatible with one another in order to provide an accurate balance of protein–water–lipid–ion interactions that allows for a complete description of ion permeation and channel gating. This is achieved by a common force field optimization strategy existing for many biomolecular force fields (Zhu *et al.* 2012) as well as thorough testing of force field combinations (Cordomí *et al.* 2012).

One pertinent challenge with ion channel MD simulations has to do with the optimal combination of ion van der Waals (vdW) force field parameters with those for proteins, lipids and other ions. The problem arises from the fact that ion parameters are typically optimized to reproduce ion energetics in bulk water, but do not necessarily provide accurate estimates for their direct interactions with other components such as lipid head groups, counterions, or the protein backbone (critical for ion conduction in K^+ channels). Thus, development of vdW parameters for specific interactions involving ions has been performed (see, e.g. Berneche & Roux, 2001; Luo & Roux, 2009; Venable *et al.* 2013; Kahlen *et al.* 2014; Li *et al.* 2015). However, direct experimental reference values, such as ion solvation energetics, are either not well defined (absolute ionic solvation free energy values are defined relative to unknown H^+ solvation energetics), or not available. Therefore, surrogate markers, such as

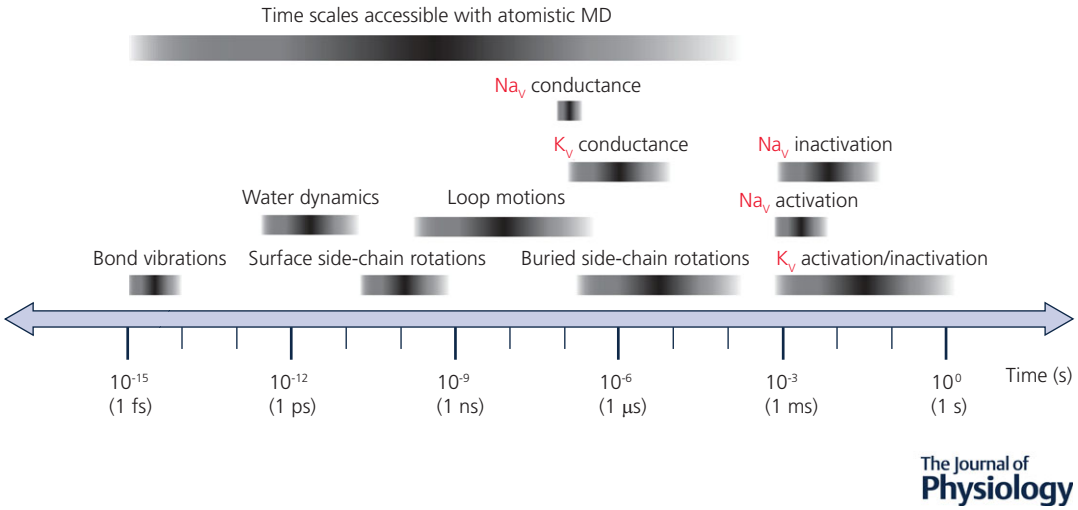

Figure 3. Time scales accessible with atomistic MD simulations and those related to ion channel function (gating and permeation, estimated based on IUPHAR/BPS data; Southan *et al.* 2016) as well as protein and solvent dynamics (adapted from Lindahl, 2008; Zwier & Chong, 2010; Harvey & De Fabritiis, 2012)
The fastest molecular motions in a simulated system are bond and angle vibrations (on the fs time scale) and serve as an upper limit of MD time step. A lower time limit of ion channel activation/inactivation transition at ~1 ms practically coincides with an upper time limit of atomistic MD simulations.

experimental salt solubilities (Yu *et al.* 2010), ion pair formation/dissociation constants (Kahlen *et al.* 2014), salt solution osmotic pressures (Luo & Roux, 2009) and charged membrane electrophoretic mobilities (Venable *et al.* 2013), typically combined with gas-phase and/or condensed-phase QM calculations are used instead.

The application of such special pairwise ion vdW parameter terms (force field patches) should, in principle, provide a more accurate description of different interactions in biomolecular systems and thus better agreement with experimentally determined values for ion permeation mechanisms and kinetics. However, no consistent picture has emerged so far. For instance, in one study the presence or absence of such a CHARMM force field patch had inconsistent results on ion permeation mechanisms for different channels (KcsA and $K_V1.2/K_V2.1$ chimera), and did not improve underestimated computed ion conductance values (Jensen *et al.* 2013). In another recent study, a choice of different ion parameters without special vdW terms, but optimized to be used with Amber and CHARMM biomolecular force fields, respectively, resulted in similar permeation mechanisms but substantially faster K^+ conduction rates in KcsA for the former (Köpfer *et al.* 2014). In Na_V channel simulations, different choices of ion parameters with and without pairwise vdW parameter patches resulted in reasonable agreement between experimental and computed ion conductances (Ing & Pomes, 2016), likely due to substantially wider SF and thus weaker ion–protein interactions in those channels (see below). What many studies agree on is that the absence of explicit electronic reorganization in classical force field-based MD simulations can lead to overestimated ion permeation barriers, and thus reduced computed conductances, especially for channels with narrow pores (Allen *et al.* 2006; Jensen *et al.* 2013). Unfortunately, at this time explicit representation of electronic degrees of freedom, as done in QM calculations, is impossible due to the large size of biomolecular systems and the associated exorbitant computational cost. Similarly, a hybrid approach that combines empirically derived molecular-mechanical (MM) force fields with QM (known as QM/MM) can only reach picosecond time scales (Bucher & Rothlisberger, 2010) due to computational complexity.

An alternative to using QM or QM/MM is to use polarizable force fields in MD, where electronic degrees of freedom are approximated by auxiliary charged particles (known as Drudes), variable point multipoles, or restrained fluctuation of atomic charges in the field of other atoms (MacKerell, 2004; Lopes *et al.* 2015). Unlike classical fixed-charge force fields, they allow for a substantial variation of a molecular electrostatic response in media of different polarities and thus potentially more accurate intermolecular interactions. For instance, in these models, the non-polar environment of the membrane interior has a correct dielectric constant of around 2, allowing for accurate solvation of charged and polar species (Vorobyov *et al.* 2008). Despite the complications associated with parameterization of polarizable force fields, and higher computational overhead for MD runs, hybrid polarizable/additive and fully polarizable models have been used for prototypical gramicidin A ion channel simulations (Allen *et al.* 2004; Patel *et al.* 2009; Vorobyov *et al.* 2010; Peng *et al.* 2016), demonstrating reduced free energy barriers and thus providing more accurate channel conductance. And, fully polarizable MD simulations were reported recently for other ion channels as well (Dhakshnamoorthy *et al.* 2016; Kratochvil *et al.* 2016; Sun & Gong, 2017).

Here we will focus on the application of atomistic MD to the study of the processes of ion conduction and gating of K^+ and Na^+ ion channels, and we will discuss recent challenges and breakthroughs in the field as they relate to physiology.

Ion conduction

Ion movement across K^+ channel selectivity filter

Selectivity filter structure is intimately tied to its function. The SFs of some K^+ channels are responsible for the channels' 10,000-fold preference for K^+ over Na^+ (not explicitly discussed in this paper; see Roux, 2017 for a recent review) and can facilitate the flux of 10^8 K^+ ions per second (Hille, 2001) across a membrane. The SFs of such K^+ channels as KcsA, K_VAP and $K_V1.2$ are narrow passageways that are lined with the backbone atoms of the highly conserved TVGYG amino acid sequence (Doyle *et al.* 1998; Lee *et al.* 2005; Long *et al.* 2005*a*). Within the SF four cage-like binding sites, $Site_1$–$Site_4$, have been identified via crystallography (Morais-Cabral *et al.* 2001) and two more sites, $Site_0$ and $Site_{cav}$, located just above and just below the SF, respectively, have been elucidated via MD simulations (Aqvist & Luzhkov, 2000; Berneche & Roux, 2001). Despite putative agreement on the structure of the SF, the original crystallographic evidence leaves room for interpretation of the ion occupancy in the filter region. Distinct occupancy patterns that depend on the presence of water molecules between the adjacent ions give rise to several proposed mechanisms whereby ions traverse the narrow constriction of the SF (Köpfer *et al.* 2014; Kratochvil *et al.* 2016).

Proposed mechanisms of K^+ conduction. The historically prevailing computational and experimental evidence has asserted that water molecules reside between adjacent ions in the SF. The KcsA X-ray crystal structure confirmed the presence of at least two ions in the SF (Doyle *et al.* 1998), supporting a model of permeation known as the knock-on mechanism, originally proposed by Hodgkin

& Keynes (1955). This mechanism (Morais-Cabral *et al.* 2001) is reinforced by MD simulations, and proposes that two ions are initially in positions [$Site_3$, $Site_1$], separated by water molecules (Fig. 4*A*). As a third ion enters the $Site_{cav}$ below the SF (not labelled in the figure), an intermediate configuration of ions in [$Site_4$, $Site_3$, $Site_1$] forms, at which point K^+ in position $Site_4$ 'knocks on' the entire single-file assembly of ions, causing it to undergo a concerted movement, such that the potassium ions end up in positions [$Site_4$, $Site_2$] (Aqvist & Luzhkov, 2000; Berneche & Roux, 2001; Bernèche & Roux, 2003).

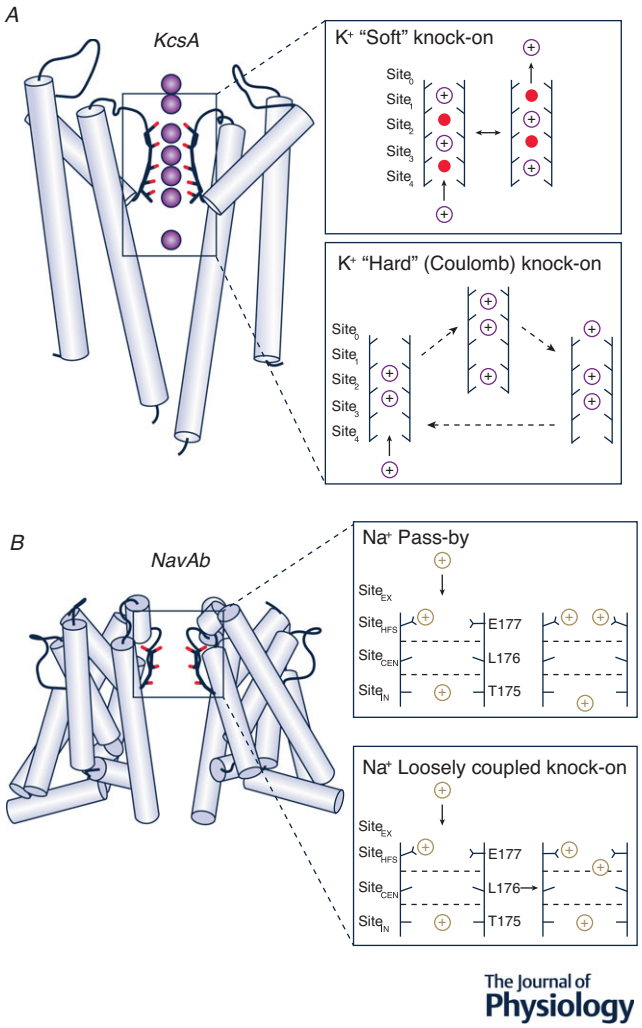

Figure 4. Ion channel conduction mechanisms
A, KcsA crystal structure (Zhou *et al.* 2001) (PDB ID: 1K4C, left) with crystallographic ion positions shown by purple spheres, α-helices by light-blue cylinders, loops by black curves and ion/water coordinating SF oxygen atoms by red sticks. The insets on the right demonstrate K^+ conductance 'soft' knock-on (Berneche & Roux, 2001) (top) and 'hard' or Coulomb knock-on (Köpfer *et al.* 2014) (bottom) mechanisms. K^+ ions shown in purple, water molecules shown in red; putative ion occupancy positions in each SF are labelled $Site_0$–$Site_4$. $Site_{cav}$ is located below the SF and is not shown on the diagrams. *B*, Na_VAb crystal structure (Payandeh *et al.* 2011) (PDB ID: 3RVY, left) with α-helices shown by light-blue cylinders, loops by black curves and ion/water coordinating SF oxygen atoms by red sticks. The insets on the right demonstrate Na^+ conductance by pass-by (top) and loosely coupled knock-on (bottom) mechanisms for prokaryotic Na_V channels (Boiteux *et al.* 2014). Na^+ ions are shown in brown, water molecules are not shown for clarity, and putative ion occupancy positions in each SF are labeled $Site_{EX}$, $Site_{HFS}$, $Site_{CEN}$ and $Site_{IN}$.

Uncertainty in the crystallographic interpretation of KcsA SF occupancy (Zhou & MacKinnon, 2003; Sheldrick, 2015) as well as suggestions from MD simulations that multiple ion pathways may exist (Berneche & Roux, 2001; Furini & Domene, 2009; Fowler *et al.* 2013) encouraged a second look at the mechanism of conduction. The difference between the conventionally accepted 'soft' knock-on and Coulomb (direct or 'hard') knock-on mechanisms is the absence of the intervening water molecules for the latter (Fig. 4*A*). Initially K^+ ions are found in $Site_3$ and $Site_2$. As the third ion fluctuates between $Site_{cav}$ and $Site_4$ binding sites, it directly knocks on the ions above, pushing them into [$Site_2$, $Site_1$] as a result of direct electrostatic repulsion. According to 1D reduced-representation model calculations, the conductance calculated on the basis of the Coulomb knock-on mechanism is in much closer agreement with experiment (Köpfer *et al.* 2014). The plausibility of such a mechanism is still being debated, with a recent combined spectroscopic–MD study suggesting a better agreement for a traditional 'soft' knock-on mechanism (Kratochvil *et al.* 2016), and an improved crystal structure refinement method pointing to the direct Coulomb knock-on (Sheldrick, 2015). In a recent study, the authors performed multiple multi-microsecond MD simulations on several K^+ channels and argued that only the Coulomb knock-on mechanism can account for a high conduction efficiency and K^+/Na^+ selectivity through direct interaction of completely dehydrated K^+ ions in the SF (Kopec *et al.* 2018). What should be noted, however, is that the outcome of these simulations ultimately depends on the specific ion, water and protein force field parameters employed, discussed above and also mentioned in previous studies (Jensen *et al.* 2013; Köpfer *et al.* 2014). Moreover, a mechanism of ion permeation will likely depend on the specific channel as well as experimental conditions such as salt concentrations and applied voltages. In the majority of unbiased MD simulations to date, substantially higher voltages (hundreds of millivolts) and ion concentrations (e.g. 0.3–0.6 M) compared to physiological values (tens of millivolts and up to 0.15 M) have been used to observe ion conduction at the microsecond time scale (Jensen *et al.* 2013; Köpfer *et al.* 2014; Kopec *et al.* 2018). So, a direct correlation between MD and cell-based electrophysiology measurements is not clear. Additional high-resolution experimental data and MD simulations using accurate empirically derived models of water, ion and protein interactions will likely help resolve this controversy.

Ion movement across Na^+ channel selectivity filter

Na^+ binding sites from experimental structures and MD simulations. The last half a decade has seen a proliferation of voltage-gated sodium channel crystal structures. A few examples are the Na_VAb channel from *Arcobacter butzleri* crystallized in putative open and closed states (Payandeh *et al.* 2011; Lenaeus *et al.* 2017), Na_VMs from *Magnetococcus marinus,* likely in the open state (Sula *et al.* 2017) and Na_VRh, from *Rickettsiales* sp. HIMB114, likely in an inactivated state (Zhang *et al.* 2012). A common element among the three channels is the structure of the SF region, which is composed of helix–loop–helix motif. The Pore 2 helix (P2) forms an electronegative funnel-shaped opening to the extracellular region, attracting ions into the pore, whereas the ion selection itself takes place mostly in the loop region. Amino acid sequences of the loop differ among the various channels, but bacterial Na_V channels contain a highly conserved glutamic acid (Glu) residue in every subunit, forming a Glu ring (EEEE) around the dominant, high-field-strength Na^+ binding site, $Site_{HFS}$, or $Site_1$ (Fig. 4*B*) near the mouth of the SF (Clairfeuille *et al.* 2017). In multiple MD simulations of a closed Na_VAb ion channel, two dominant Na^+ binding sites were identified (Ing & Pomes, 2016). In $Site_{HFS}$, Na^+ was found in the octahedral coordination, bound directly by carboxylates of two Glu side chains, by water molecules H-bonded to the two other Glu residues, as well as by two more water molecules from aqueous environment of the vestibule. The second dominant site, referred to as $Site_{IN}$ or $Site_3$, is located deeper in the SF. Here Na^+ sits in an almost square planar arrangement, coordinated by four water molecules H-bonded to nearby threonine carbonyls and by a water from above. A less favourable, off-axis $Site_{CEN}$ or $Site_2$ site has been isolated as well (Carnevale *et al.* 2011). The substantially wider pore of Na_V channels creates a very different conduction environment from a single-file ion/water arrangement in the SF of K^+ channels.

Proposed mechanisms of Na^+ conduction. An early MD simulation of Na_VAb ion translocation proposed a 'loosely coupled knock-on' with a low permeation barrier for two-ion occupancy of the SF (Corry & Thomas, 2012). Several subsequent studies confirmed initial findings and also proposed a three-ion analogue (Fig. 4*B*) (Ing & Pomes, 2016). A more standard, concerted, knock-on mechanism, with two sodium ions in the SF of Na_VAb, has also been reported (Chakrabarti *et al.* 2013). In both cases, as the next ion approaches the external $Site_{EX}$ or $Site_0$, it knocks on the filter-dwelling ions pushing them farther down into the SF or to the central cavity. An observation of two sodium ions simultaneously occupying the same binding site, i.e. a 'pass-by' configuration, has been also noted (Chakrabarti *et al.* 2013; Boiteux *et al.* 2014), made possible by the width of the selectivity filter and the number of available coordinating ligands (Fig. 4*B*). Both rotameric and protonation states of the Glu side chains forming the $Site_{HFS}$ have been shown to impact conduction. Conformational isomerization may distort this critical site, while protonating one or more Glu side chains was found to reduce or abolish conduction altogether (Ing & Pomes, 2016). Recently, a putative open-state crystal structure of Na_VAb/1-226 construct with nearly identical SF geometry was published (Lenaeus *et al.* 2017), reaffirming the findings from the previous closed-state studies. In a microsecond-long MD simulation of ion translocation through an open Na_VMs pore, five presumed Na^+ binding SF sites, $Site_0$–$Site_4$, were identified as well (Ulmschneider *et al.* 2013) in good agreement with Na_VAb closed-channel structure and simulations. Such consensus points to a possible common structural mechanism for bacterial Na_V channel conduction, but it requires further work for complete elucidation.

Eukaryotic Na_V channels have a different architecture with four homologous domains (DI–DIV) on a single polypeptide chain instead of four identical subunits in bacterial channels. Cryo-EM structures of eukaryotic sodium channels, Na_VPaS from cockroach (Shen *et al.* 2017) as well as $Na_V1.4$ from electric eel (Yan *et al.* 2017) and human (Pan *et al.* 2018), have recently been determined. Their SFs display asymmetries with aspartic acid, glutamic acid, lysine and alanine (DEKA) from different channel domains forming Na^+ binding site $Site_{HFS}$ compared to the EEEE ring in prokaryotic channels. Several recent MD studies used eukaryotic Na_V homology models (Mahdavi & Kuyucak, 2015; Ahmed *et al.* 2017), hybrid models with a grafted SF eukaryotic Na_V channel SF onto bacterial structures (Li *et al.* 2017*b*; Flood *et al.* 2018) as well as new Na_VPaS structure (Zhang *et al.* 2018). These studies identified a unique asymmetric Na^+ permeation pathway involving coordination with Asp and Glu residues in the DEKA ring as well as in the outer SF. A cationic Lys residue in the DEKA ring was also found to be crucial for the Na^+ conduction mechanism and Na^+/K^+ selectivity in those studies, in particular participating in the knock-on mechanism similarly to a permeating Na^+ ion (Flood *et al.* 2018). No doubt future studies of the structural differences between prokaryotic and eukaryotic ion channels will bring about new understanding of ion permeation in sodium channels of different organisms, but extrapolating these findings to eukaryotic Na_V channel function due to their complexities remains a formidable task.

Connecting MD ion permeation with experiment

In MD simulations of ion channels, it is essential not only to elucidate the molecular mechanisms of ionic permeation across the SF but also to establish

a connection with experimental observables such as the ionic current–voltage (*I–V*) relationship and the single channel conductance values derived from them (Hille, 2001). Physiologically, membrane voltage arises from different ion concentrations on both sides of the membrane. However, MD simulations of ion channels in hydrated lipid bilayers with periodic boundary conditions preclude any variation of ionic strength between the intra- and extracellular environments. One way to circumvent this difficulty is to design a dual bilayer system stacking the two membranes in the *z* direction and creating two separate aqueous compartments: one on the outside of both bilayers and the second one between them (Kutzner *et al.* 2011). An ion/water exchange between the compartments is carried out to maintain the desired ion gradient throughout the simulation. Application of this method to KcsA, MthK and $K_V1.2$ channels yielded good agreement with experiment (Kutzner *et al.* 2016). Another approach is to apply an extra force, proportional to the electric field, to every charged atom in the system. The resultant voltage can be computed as a product of the electric field and the size of the simulation box (Gumbart *et al.* 2012). This technique was applied to $K_V1.2$–2.1 chimera, but under physiologically relevant membrane voltage, the conductance was found to be almost 40-fold below the experimental value (Jensen *et al.* 2013). This does not mean that this approach is inferior to a dual-bilayer set-up and, in principle, should provide comparable results. In fact, simulations of an open Na_VM_S channel pore using the constant electric field method provided a reasonable agreement with experiment (Ulmschneider *et al.* 2013). The sources of differences can be manifold (Fowler *et al.* 2013), ranging from different simulation protocols or convergences to the force field parameters, which can alter a fine balance of different intermolecular interactions and thus permeation mechanisms and kinetics. The latter factor is still important but arguably may be less sensitive for Na_V channels due to the relatively wider pores.

Notable disparity between theoretical and computational results may be rooted in the inherent differences in mechanical and chemical properties arising from system lipid composition. MD systems usually focus on an ion channel in a single-lipid membrane patch, often omitting heterogeneity and asymmetry of membranes. The importance of lipid composition for proper ion channel function is well known experimentally and via MD simulations, e.g. for KcsA (Valiyaveetil *et al.* 2002; Deol *et al.* 2006; Marius *et al.* 2008; Rusinova *et al.* 2014) and K_V channels (Schmidt *et al.* 2006; Abderemane-Ali *et al.* 2012; Rodriguez-Menchaca *et al.* 2012; Kasimova *et al.* 2014; Yazdi *et al.* 2016), and can possibly contribute to observed differences in experimental and computed conductances as well as channel gating mechanisms, discussed below.

Mechanisms of ion channel gating

In the K_V and Na_V families of voltage-gated cation channels (VGCCs), the voltage-dependent variation of ionic current has been associated with a gating cycle of activation/deactivation, inactivation and recovery from inactivation (Hille, 2001). This cycle depends fundamentally on voltage sensing, whereby changes in the cell membrane potential engender widening or constriction of the channel's hydrophobic pore region through the movement of VSD. One structural hypothesis is that gating is a discrete process: one in which the global conformational transition between VSD-activated and deactivated states causes the S6 helices of the PD to either open or close the ion passageway. The pore closing transition is often accompanied by dewetting of the hydrophobic region, and aqueous pore stability increases with its radius and polarities of pore-lining residues, which has been observed in MD simulations (Jensen *et al.* 2010). Thus, the narrow hydrophobic pores of many K^+ and Na^+ channels often rely on stabilizing interactions with activated VSD for VGCCs, low pH for KcsA, or artificial restraints during MD simulations of pore-only constructs.

An alternative structural hypothesis is that gating is a continuous process: one in which there are ensembles of conformations corresponding to open and closed states, as opposed to singular open or closed ion channel conformations. In their work on neuronal Na^+-activated K^+ channels, Hite and MacKinnon found that there is an ensemble of structures representative of non-conductive states that are in $[Na^+]$-dependent equilibrium with a structure exhibiting an open, conducting conformation (Hite & MacKinnon, 2017). Additionally, a recent MD study on the pore domain of K_VAP identified a distinct free energy minimum, corresponding to a possible stable intermediate state, along the gating pathway between open and closed states of the channel (Starek *et al.* 2017). A description of other recent MD simulation findings on the K^+ and Na^+ channel gating including both inactivation and deactivation phenomena is provided below.

N- and C-type inactivation

Upon prolonged depolarization, VGCCs can undergo conformational changes that usher them into a non-conducting, inactivated state, in which the channel is desensitized to membrane voltage perturbations, either through intracellular pore block (fast or N-type inactivation) or through a SF distortion (slow or C-type inactivation), as illustrated in Fig. 5. In K_V channels such as ones in the Shaker family, a ball-and-chain or hinged-lid mechanism of N-type inactivation has been proposed (Zagotta *et al.* 1990), where N-terminal residues on the cytoplasmic side of the channel comprising ball and chain domains of one chain can occlude the channel pore. In

eukaryotic Na_V channels N-type inactivation has been mainly thought to occur via a pore occlusion by the cytoplasmic linker region between DIII and DIV, featuring an essential Ile-Phe-Met (IFM) sequence (DeMarco & Clancy, 2016), and is responsible for the rapid cessation of Na^+ conduction during the upstroke of the action potential. So far, study of the molecular determinants of N-type inactivation via molecular simulations has remained out of reach, largely due to a lack of structural data. However, the recently resolved structures of electric eel and human $Na_V1.4$ channels in presumably the inactivated state with intact IFM motif (Yan *et al.* 2017; Pan *et al.* 2018) will likely lead to more thorough and detailed MD studies of this phenomenon.

C-type inactivation in K^+ channels, illustrated in Fig. 5, has been investigated extensively in experimental structural and functional studies, as well as atomistic simulations, and several possible contributing factors have been analysed. Typically, SF distortions have been considered as a key feature of C-type inactivation (Hoshi *et al.* 1991; Hoshi & Armstrong, 2013). This view has been challenged by a recent experimental KcsA study employing D-Ala substitution of a critical Gly77 residue (G77dA mutation), which should have removed inactivation due to prevention of the SF backbone from buckling, but inactivation still took place for this mutant at low K^+ concentration (Devaraneni *et al.* 2013). However, a 1.2 μs unbiased and 2D umbrella sampling MD simulation study of the same G77dA mutant demonstrated that the underlying premise of D-Ala propping the SF open was not accurate (Li *et al.* 2017*a*), supporting the notion that SF distortion is indeed a hallmark of C-type inactivation.

Structurally, one supposition is that polar interactions behind the SF stabilize the inactivated state. This idea is corroborated by computational and experimental studies of KcsA, in which Glu71(H^+)–Asp80 carboxyl/carboxylate interaction was observed, leading to a 'pinched' SF conformation, eliminating K^+ binding sites $Site_2$ and $Site_3$, and thus abolishing channel conductance (Cordero-Morales *et al.* 2006; Cuello *et al.* 2010*b*). This is similar to KcsA behavior in a low-[K^+] environment, which leads to SF pinching, making site $Site_2$ inaccessible and $Site_1$, $Site_3$, and $Site_4$ filled with water molecules according to MD simulations (Boiteux & Berneche, 2011). Earlier MD simulations of KcsA with an outwardly flipped SF Val76 backbone carbonyl also related it to inactivation (Berneche & Roux, 2005), although a recent combined spectroscopic/MD study suggests that such a flipped state for this channel can be an integral component of the ion permeation process with about 40% occurrence (Kratochvil *et al.* 2016). Interactions of SF with water molecules buried behind may induce a long-lasting C-type inactivated state as well, requiring their removal and rebinding of external K^+ to promote the recovery process (Ostmeyer *et al.* 2013). The crucial role of these water molecules is reinforced by their presence in a recent crystal structure of a fast-inactivating Y82A KcsA mutant with a SF collapse at Site2 and Site3 due to Gly77 and Val76 backbone movements (Cuello *et al.* 2017).

An alternative explanation of C-type inactivation involves either SF dilatation at the K^+ binding site $Site_1$ (Hoshi & Armstrong, 2013), or a constriction of the SF at $Site_4$ (Pau *et al.* 2017), leading to its partial dehydration and corresponding loss of an efficient knock-on mechanism.

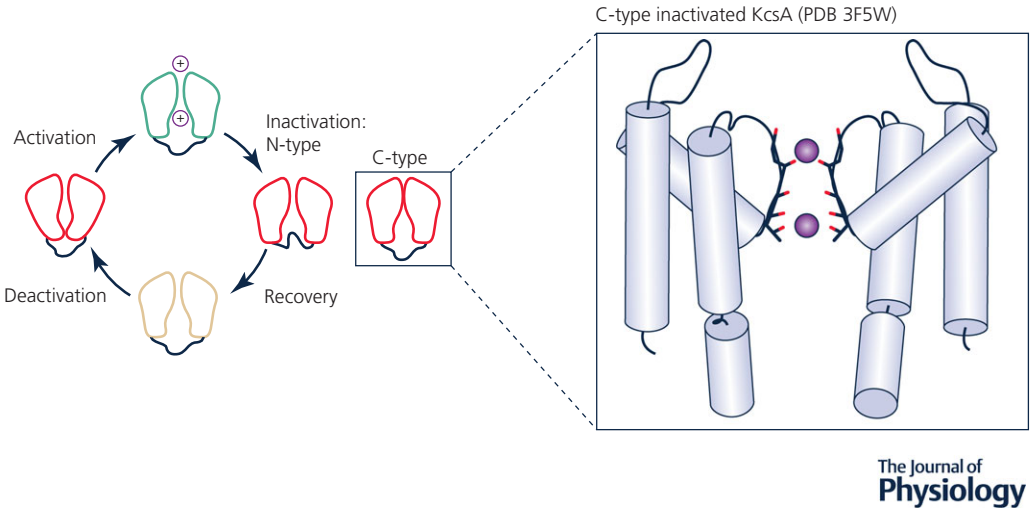

Figure 5. Ion channel gating cycle
Activation/deactivation, C-type and N-type inactivation and recovery from inactivation (Rasmusson *et al.* 1998). A structure representing a putative C-type inactivated state for the KcsA channel (Cuello *et al.* 2010*b*) (PDB ID: 3F5W) is shown as an inset. Crystallographic ion positions are shown by purple spheres, α-helices by light-blue cylinders, loops by black curves and ion/water coordinating SF oxygen atoms by red sticks.

A recent combined MD and experimental study of the Shaker K_V channel demonstrated that the SF widening associated with C-type inactivation is a result of the pore domain being pulled outward towards the VSD (Conti *et al.* 2016). This study revealed a tight coupling between voltage-induced activation, S4 helix movement and pore widening due to S6 rotation, leading to a concerted centrifugal motion of Glu416 at the top of S5 helix causing SF dilation and the loss of K^+ binding (Conti *et al.* 2016). Such a mechanism is clearly impossible in KcsA since it completely lacks a voltage-sensing domain, but a direct correlation between pore opening at the intracellular gate and SF K^+ coordination was observed in a crystallographic study (Cuello *et al.* 2010*a*) and explored further via MD simulations (Pan *et al.* 2011) and solid-state NMR (Xu *et al.* 2017). Phe103 on the inner helix was shown to play a crucial role in allosteric coupling between proton binding at the intracellular pH sensor and K^+ loss from the SF promoting inactivation (Xu *et al.* 2017).

A very recent multi-microsecond MD study of KcsA has shown that there is a single free-energy minimum corresponding to a partially open intracellular gate and a conductive SF (Li *et al.* 2018). In this work, the authors examined the conformational dynamics of the SF and corresponding interactions with associated ions and water in closed, intermediate and open states of the channel. They observed that the gating conformation of the pore is allosterically coupled to the spontaneous constriction in the SF at Gly77, induced by the rotation of the peptide bond between Gly77 and Val76 (Delemotte, 2018; Li *et al.* 2018), and that this constriction coincides with the infiltration and binding of three water molecules in the region behind the SF, which was observed in a previous MD study (Li *et al.* 2017*a*) and a recent crystal structure (Cuello *et al.* 2017). Furthermore, another recent combined MD simulation/experimental study of KcsA has suggested that the SF might actually act as the primary gate in certain K^+ channels, and that some SF relaxation is necessary for ion conduction, with the interactions between outer transmembrane helix TM1 and P-helix playing important role in this process (Heer *et al.* 2017).

MD simulations are also helping to identify possible mechanisms of C-type inactivation in voltage-gated sodium channels. A distortion of the SF coupled to S6 helix bending in Na_VAb was observed over the course of microsecond-long MD simulations (Boiteux *et al.* 2014), and is supported by the existence of crystal structures of putative C-type inactivated conformations of Na_VAb, which show a dimer-of-dimers configuration of the pore domain and SF as well (Payandeh *et al.* 2012). However, it is not clear if the SF distortions discussed above are directly related to inactivation. It is also possible that the thermodynamic instabilities observed in simulations are either due to inherent channel sub-conducting states, or MD force field parameters. Substantially longer experimental time scales of channel inactivation compared to accessible atomistic MD simulation times (see Fig. 3) make a direct observation of a conformational transition from stably conducting to an inactivated state of K^+ or Na^+ channels not feasible unless an experimental structure, simulation conditions or force field parameters would predispose for it. And determining a major underlying cause of observed channel conducting and inactivated state stabilities and structural mechanisms of their transitions in between is far from trivial. Hopefully, comprehensive combined experimental/MD studies in the near future will be able to resolve these issues.

Activation and deactivation

The VSD movement during VGCC activation and deactivation has been thoroughly studied for several decades both experimentally and theoretically, recently culminating in a widely accepted consensus model (Vargas *et al.* 2012). Based on a number of functional studies that were later confirmed by X-ray structures, such as that of $K_V1.2$ (Long *et al.* 2005*b*), it is well established that the S1–S4 helices of VGCCs comprise the voltage sensing domains, as illustrated in Fig. 1, with several positively charged residues of S4 (typically, arginine or lysine followed by two hydrophobic residues) acting as gating charge carriers. Experimentally, a transient current across the capacitive membrane is measured, which, when integrated over time, reveals total macroscopic gating charge transported across the membrane (ΔQ) associated with the conformational change of the voltage sensor. Single channel conductance measurements and computer modelling studies estimated ΔQ to be ~12–14e (Aggarwal & MacKinnon, 1996; Seoh *et al.* 1996; Bezanilla, 2000; Pathak *et al.* 2007) for the Shaker K^+ channel. Many models of voltage sensing were developed, and MD simulations have been used to study their viability.

Helical screw and sliding 3_{10}-helix models of voltage sensing. Over time, structural data led to the development of a model in which S4 was presumed to be a transmembrane α-helix in both resting and activated states, with the positively charged S4 residues forming a series of ionic pairs with neighbouring residues in the surrounding S1–S3 helices that stabilize the VSD in different stages upon depolarization (Durell *et al.* 2004; Chen *et al.* 2010). The translocation of the S4 helix of the VSD was experimentally determined to involve the charged S4 residues passing, in steps, by a conserved phenylalanine residue that serves as a gating charge transfer centre (Tao *et al.* 2010). In a model known as the helical screw, the S4 α-helix was proposed to translate ~13.5 Å and rotate a total of 180° in three steps, in a screw-like motion (Grizel *et al.* 2014) (Fig. 6 top). This model is illustrated by a recently resolved crystal

structure of a voltage-sensitive phosphatase from *Ciona intestinalis* (Ci-VSP). Superimposition of its VSD with that of Na_VAb and $K_V1.2$ showed S4 movement being consistent with that of an α-helical screw, and the gating charge transfer computed through MD simulation agreed with experiment (Li *et al.* 2014).

Within the hydrophobic region of the VSD, S4 can also adopt a unique secondary structural element known as a 3_{10}-helix, which has been observed in crystal structures (Long *et al.* 2007) and also predicted in several molecular modelling studies (Vargas *et al.* 2012; Yarov-Yarovoy *et al.* 2012). A 3_{10}-helical configuration changes the pattern of alternating charged residues on the S4 voltage sensor, allowing for a vertical translation of 2.0 Å per amino acid, as opposed to 1.5 Å for an α-helix (Long *et al.* 2007), as illustrated in Fig. 6 bottom. For some time, the existence of a 3_{10}-helix in transmembrane proteins was extremely controversial, because they were rarely seen in membrane protein crystal structures due to their inherent energetic instability (Tobias & Brooks, 1991; Karpen *et al.* 1992). MD simulations were not only able to reveal that the S4 can adopt a 3_{10}-helical configuration spontaneously, but that such a structural arrangement allows for total ΔQ transfer of 10–14e (Khalili-Araghi *et al.* 2010), within the range of what has been measured experimentally. A steered MD study of the $K_V1.2$ VSD showed that the energy barrier to S4 translocation past the gating-charge transfer centre is reduced by a factor of 2 in the 3_{10}-helical configuration as opposed to an α-helical configuration, in which the S4 must turn (helical screw model) (Schwaiger *et al.* 2011). A consensus is now emerging that the 3_{10}-helix is likely the voltage-sensing element of activation in many VGCCs

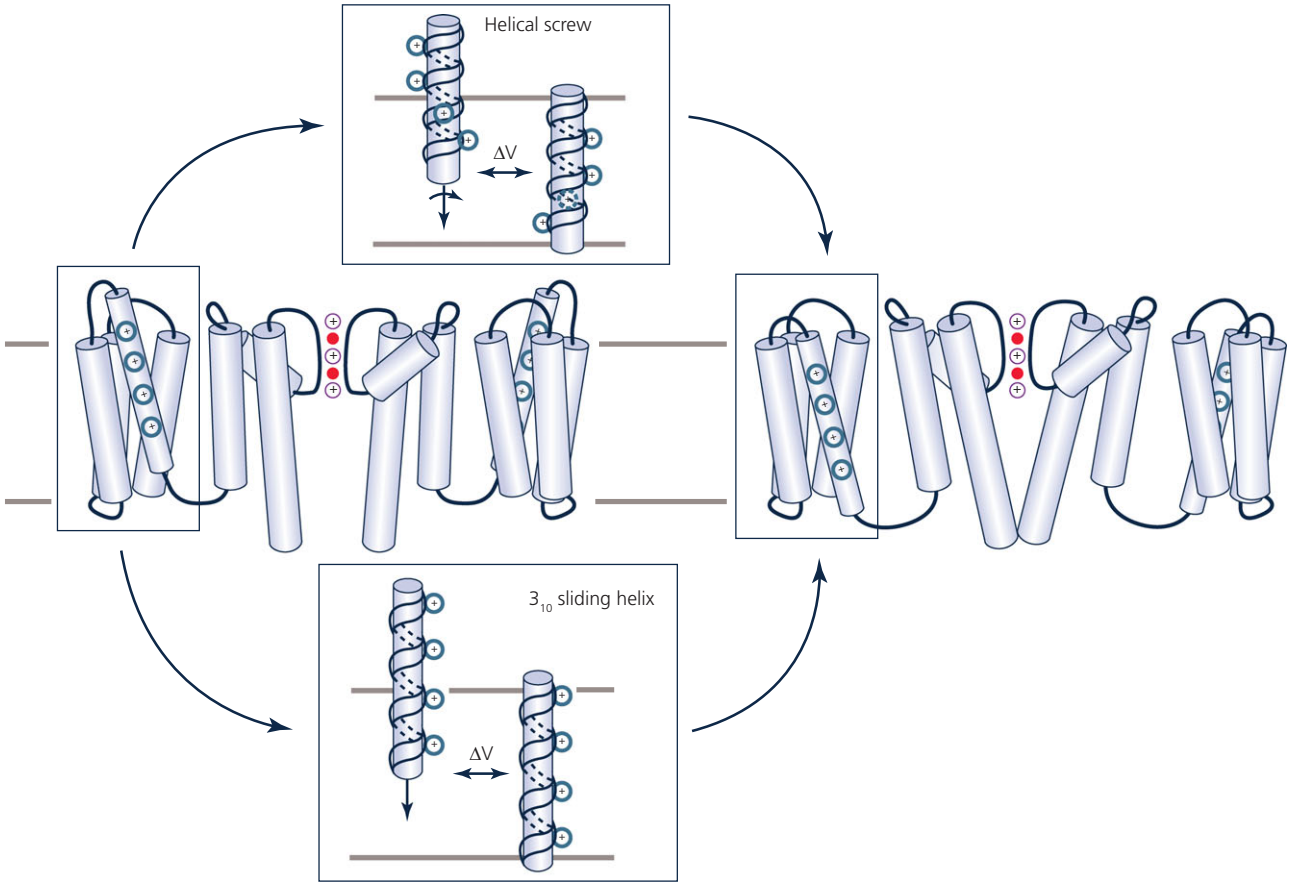

The Journal of Physiology

Figure 6. Models of voltage sensing
Voltage-gated K^+ channel model illustrated in an open pore state with activated VSD (left) and a closed pore state with resting VSD (right) based on hERG (Wang & MacKinnon, 2017) and EAG (Whicher & MacKinnon, 2016) cryo-EM structures. Top and bottom insets show proposed S4 movement models during a channel deactivation process. Top: S4 helical screw model (Grizel *et al.* 2014), with S4 shown as an α-helix, also depicting a 180° turn during activation, in a screw-like motion. Bottom: S4 3_{10}-helix consensus model (Vargas *et al.* 2012), depicting a more tightly wound 3_{10}-helix undergoing a sliding motion. Charged residues on S4 are shown in blue. See Fig. 1 for more details.

(Vargas *et al.* 2012). Its unique structural motif confirmed that the S4 basic residues were at 120° intervals on the S4 helix, consistent with early histidine scan experiments (Bezanilla, 2002). Nevertheless, the Ci-VSP structure (Li *et al.* 2014) suggests that a helical screw model should not be discounted, and that structural mechanisms of voltage sensing can vary for different VSDs.

Simulations of voltage sensor motion. When the first $K_V1.2$ structure was resolved in an open, activated configuration, efforts were made almost immediately to induce a deactivated state of the channel in MD simulation. In one study, an applied electric field of 0.052 V nm^{-1} (corresponding to a membrane potential drop of ∼500 mV) was used in an attempt to understand deactivation of $K_V1.2$; however, what was observed instead was 120° rotation of the S4 over the course of 1 μs of simulation, with little translation of the segment (Bjelkmar *et al.* 2009). Notably, however, the rotation of the S4 in such an applied electric field was coupled to the formation of a 3_{10}-helical conformation, which is longer and more tightly wound and thinner compared to an α-helix (see above), making S4 more disposed to downward motion with decreased perturbation of the rest of the VSD (Schwaiger *et al.* 2011). Since the translocation of S4 occurs on the order of microseconds, one study applied a very strong transmembrane potential drop of ∼800 mV in order to drive the voltage sensor down in an abbreviated simulation time frame (∼30 ns), and while they did not observe the formation of a 3_{10}-helix, a ∼7 Å translocation and axial rotation as in the helical-screw model was observed, with S4 going through two intermediate states corresponding to different arginine gating charge–glutamate counter charge interactions (Nishizawa & Nishizawa, 2008). Since there is a coupling between VSD movement and channel pore opening and closing, capturing a complete channel gating transition became the ultimate goal of K_V simulation studies.

In a landmark long-time-scale MD study on a special-purpose Anton supercomputer, a $K_V1.2/K_V2.1$ channel structure with an open pore and activated VSD (Long *et al.* 2007; Tao & MacKinnon, 2008) was successfully driven into a resting VSD, closed pore state on a physiological time scale of ∼200 μs at a large negative membrane potential (Jensen *et al.* 2012). In this thorough study, the authors observed the S4 helix translating ∼15 Å in total across the membrane in sequential steps, while also rotating 120°, in keeping with what had been observed in previous simulation and modelling studies. Importantly, they also observed sequential movement of S4 charged residues past the gating charge centre F233 (on the S3 helix) identified earlier (Tao *et al.* 2010), and found that the activated voltage sensors delayed pore dewetting and closure, which were observed to occur after ∼20 μs of simulation and are required for complete deactivation. The downward movement of at least one gating charge on S4 past F233 was shown to precede pore closure, and the pore was always closed before all four VSDs fully deactivate. However, the pore opening required all four VSDs to move to an activated state first, with the S4–S5 linker packing against the S6 helix. (Jensen *et al.* 2012). It should be noted that the authors observed channel pore opening but were unable to capture a complete VSD activation upon applying a large depolarizing membrane potential to the putative resting channel structure. Moreover, in order to observe channel gating transitions, they used membrane potentials of ±750 mV, an order of magnitude larger than physiological values. However, the fact that their observed structural movement is in line with a number of experimental predictions, as well as other modelling and simulation studies (Vargas *et al.* 2012), makes it reasonable to extrapolate their findings to ion channel gating behaviour in their native environment.

Mechanisms of activation and deactivation can be channel-dependent. Whether a similar structural mechanism of activation/deactivation applies to other VGCCs remains to be seen. Recently, cryo-EM structures of EAG (Whicher & MacKinnon, 2016) and hERG (Wang & MacKinnon, 2017) channels were solved with activated VSDs and closed and open pores, respectively. They exhibit a very short non-helical S4–S5 linker and lack a domain-swapped architecture commonly seen in other VGCC structures, in which the S1–S4 VSD is adjacent to the neighbouring PD S5–S6, rather than its own subunit. Therefore, it is likely that those channels have a different gating mechanism, with interactions between VSD and adjacent intracellular helix–turn–helix extensions of S6, termed C-linkers (Toombes & Swartz, 2016), or the juxtaposed intracellular N-terminal tails (Vandenberg *et al.* 2017), suggested to play an important role. In a recent experimental/MD analysis study, a rack-and-pinion type of coupling between voltage sensors and pore gates involving interactions between S4 and S5 helices was suggested to be a dominant activation process of such channels and an alternative mechanism for K_V channels in the Shaker family (Fernández-Mariño *et al.* 2018). Future MD simulations will likely be used to assess the validity of these assumptions.

In addition to structural activation/deactivation channel transitions, we need to know the underlying energetics that ultimately control the rates of those processes, and thus should provide a direct connection to electrophysiology experiments. Recently, free energy surface projections of $K_V1.2$ VSD activation have been computed from MD simulations, showing not only that the energetic barrier between resting and intermediate states of S4 activation is just ∼5 kcal mol^{-1}, but also that a voltage-independent relaxation process can occur without a change in ΔQ (Delemotte *et al.* 2015;

Delemotte *et al.* 2017). Interestingly, the same work demonstrated a nearly 0 kcal mol^{-1} end-point free energy difference when considering ΔQ as a reaction coordinate (Delemotte *et al.* 2015), indicating almost equal probabilities for resting and activated VSD states. In another recent study, a free energy profile for Na_VAb VSD transition between resting and pre-activated states was computed using both additive and Drude polarizable MD simulations, demonstrating a similar –7 kcal mol^{-1} free energy difference between end points, but a 2 kcal mol^{-1} reduced barrier for the latter model due to a more faithful reproduction of charge–charge interactions. (Sun & Gong, 2017). Possible sources of discrepancies between the $K_V1.2$ and Na_VAb studies include altered intrinsic stabilities for different channel families or end-states, as well as methodological differences; however, more information is needed to attribute such discrepancies more specifically.

Surprisingly, very similar outcomes were revealed for an isolated K_V PD energetics. A recent MD study computed almost equal stabilities of closed and open K_VAP pore states (Starek *et al.* 2017), in contrast to previous work suggesting a more stable $K_V1.2$ open PD state: by ∼7 kcal mol^{-1} (Fowler & Sansom, 2013). This discrepancy was explained by excessive water trapping within the pore domain in earlier simulations that were relatively short (Starek *et al.* 2017). All of this indicates the crucial importance of force-field selection and sufficiently long run times of simulations that aim to obtain accurate energetics and molecular mechanisms of ion channel gating. In addition, the free energy profiles for the gating transition of a complete VGCC structure still remain a formidable task. This has been recently done using coarse-grained (Kim & Warshel, 2014) or continuum-membrane (Silva *et al.* 2009) model calculations on several channel structures, also linking results to electrophysiological recordings, but atomistic MD studies of this process would be a long-sought nexus between ion channel simulations and experiments provided that necessary accuracy and sampling are achieved.

Conclusions

Atomistic ion channel simulations are essential for providing the spatial and temporal resolution needed to understand their normal biological function as well as their pathophysiological behaviour associated with channel mutations, or unwanted drug interactions that can potentially lead to deadly human disorders. For many decades, only experimental functional characterization of ion channels was possible due to lack of high-resolution channel structures, as well as limited computational resources and simulation methodology. The situation has changed markedly in the past 20 years with the dozens of X-ray and cryo-EM channel structures that have been made available, the advent of special-purpose supercomputers capable of running microseconds of fully atomistic MD simulations in less than a day, as well the ongoing development of advanced simulation techniques. Therefore, as our review shows, modern simulations are more capable than ever of predicting intricate molecular mechanisms of complex physiological phenomena such as ion channel permeation and voltage sensing that can, in turn, be validated experimentally. However, there are still unresolved issues related to the accuracy of the empirical force field models used in such simulations, and the problem is often aggravated by a lack of experimental data necessary for model parameterization and/or hypothesis testing, which can lead to contradictory results. An accurate balance of protein–water–lipid–ion interactions is needed to predict correct channel permeation and gating behaviour, but at present most ion channel simulations utilize fixed-charge force-field models that do not account for the explicit electron polarization necessary to predict ionic solvation in environments of different polarities, such as water and lipid membrane. Polarizable models that do account for this are more computationally demanding and are still in the developmental stage, but their increased use in biomolecular simulations will likely lead to more accurate predictions of ion channel permeation and gating mechanisms along with associated kinetics. The latter is essential to make a connection with electrophysiological observables, such as *I–V* curves, single-channel conductances and gating currents, where quantitative agreement has been achieved in some, but not all, cases, owing in large part to the accuracy limitations discussed above.

Moreover, the sampling enhancements now attainable with new computing hardware, and special simulation techniques will allow for longer simulation times, and inevitably provide a better connection to experiments as well, hence improving the predictive power of MD simulations in general. In particular, significant advancement is likely to be made in computing kinetic information for physiological processes that cannot easily be determined experimentally, such as ion channel gating, and state-specific drug binding (entry) and unbinding (egress) rates. This type of simulation-derived data can potentially be used to generate parameters for many of the function-scale models used in predictive physiology, pathophysiology and pharmacology (Silva *et al.* 2009; Yarov-Yarovoy *et al.* 2014; Clancy *et al.* 2016). We conclude that while many challenges and limitations in the field still exist, atomistic simulations of ion channels are entering a golden era of theoretical understanding and biomedical application, and although controversial findings and differing viewpoints will likely linger, such discourse is indispensable for moving the field forward.

References

Abderemane-Ali F, Es-Salah-Lamoureux Z, Delemotte L, Kasimova MA, Labro AJ, Snyders DJ, Fedida D, Tarek M, Baro I & Loussouarn G (2012). Dual effect of PIP2 on Shaker potassium channels. *J Biol Chem* **287**, 36158–36167.

Aggarwal SK & MacKinnon R (1996). Contribution of the S4 segment to gating charge in the Shaker K^+ channel. *Neuron* **16**, 1169–1177.

Ahmed M, Hasani HJ, Ganesan A, Houghton M & Barakat K (2017). Modeling the human Nav1. 5 sodium channel: structural and mechanistic insights of ion permeation and drug blockade. *Drug Des Devel Ther* **11**, 2301.

Allen MP & Tildesley DJ (1987). *Computer Simulation of Liquids*. Oxford University Press, Oxford.

Allen TW, Andersen OS & Roux B (2004). Energetics of ion conduction through the gramicidin channel. *Proc Natl Acad Sci U S A* **101**, 117–122.

Allen TW, Andersen OS & Roux B (2006). Ion permeation through a narrow channel: using gramicidin to ascertain all-atom molecular dynamics potential of mean force methodology and biomolecular force fields. *Biophys J* **90**, 3447–3468.

Aqvist J & Luzhkov V (2000). Ion permeation mechanism of the potassium channel. *Nature* **404**, 881–884.

Berendsen H, Grigera J & Straatsma T (1987). The missing term in effective pair potentials. *J Phys Chem* **91**, 6269–6271.

Berneche S & Roux B (2001). Energetics of ion conduction through the K^+ channel. *Nature* **414**, 73–77.

Bernèche S & Roux B (2003). A microscopic view of ion conduction through the K^+ channel. *Proc Natl Acad Sci U S A* **100**, 8644–8648.

Berneche S & Roux B (2005). A gate in the selectivity filter of potassium channels. *Structure* **13**, 591–600.

Bezanilla F (2000). The voltage sensor in voltage-dependent ion channels. *Physiol Rev* **80**, 555–592.

Bezanilla F (2002). Voltage sensor movements. *J Gen Physiol* **120**, 465–473.

Bjelkmar P, Niemela PS, Vattulainen I & Lindahl E (2009). Conformational changes and slow dynamics through microsecond polarized atomistic molecular simulation of an integral Kv1.2 ion channel. *PLoS Comput Biol* **5**, e1000289.

Boiteux C & Berneche S (2011). Absence of ion-binding affinity in the putatively inactivated low-[K^+] structure of the KcsA potassium channel. *Structure* **19**, 70–79.

Boiteux C, Vorobyov I & Allen TW (2014). Ion conduction and conformational flexibility of a bacterial voltage-gated sodium channel. *Proc Natl Acad Sci U S A* **111**, 3454–3459.

Bowers KJ, Chow DE, Xu H, Dror RO, Eastwood MP, Gregersen BA, Klepeis JL, Kolossvary I, Moraes MA & Sacerdoti FD (2006). Scalable algorithms for molecular dynamics simulations on commodity clusters. In SC '06: Proceedings of the 2006 ACM/IEEE Conference on Supercomputing, https://doi.org/10.1109/SC.2006.54. IEEE.

Brooks BR, Brooks III CL, Mackerell Jr AD, Nilsson L, Petrella RJ, Roux B, Won Y, Archontis G, Bartels C & Boresch S (2009). CHARMM: the biomolecular simulation program. *J Comput Chem* **30**, 1545–1614.

Bucher D & Rothlisberger U (2010). Molecular simulations of ion channels: a quantum chemist's perspective. *J Gen Physiol* **135**, 549–554.

Carnevale V, Treptow W & Klein ML (2011). Sodium ion binding sites and hydration in the lumen of a bacterial ion channel from molecular dynamics simulations. *J Phys Chem Lett* **2**, 2504–2508.

Case DA, Cheatham TE 3rd, Darden T, Gohlke H, Luo R, Merz KM Jr, Onufriev A, Simmerling C, Wang B & Woods RJ (2005). The Amber biomolecular simulation programs. *J Comput Chem* **26**, 1668–1688.

Chakrabarti N, Ing C, Payandeh J, Zheng N, Catterall WA & Pomès R (2013). Catalysis of Na^+ permeation in the bacterial sodium channel Na_VAb. *Proc Natl Acad Sci U S A* **110**, 11331–11336.

Chen X, Wang Q, Ni F & Ma J (2010). Structure of the full-length Shaker potassium channel Kv1.2 by normal-mode-based X-ray crystallographic refinement. *Proc Natl Acad Sci U S A* **107**, 11352–11357.

Clairfeuille T, Xu H, Koth CM & Payandeh J (2017). Voltage-gated sodium channels viewed through a structural biology lens. *Curr Opin Struct Biol* **45**, 74–84.

Clancy CE, An G, Cannon WR, Liu Y, May EE, Ortoleva P, Popel AS, Sluka JP, Su J, Vicini P, Zhou X & Eckmann DM (2016). Multiscale modeling in the clinic: drug design and development. *Ann Biomed Eng* **44**, 2591–2610.

Colatsky T, Fermini B, Gintant G, Pierson JB, Sager P, Sekino Y, Strauss DG & Stockbridge N (2016). The Comprehensive in Vitro Proarrhythmia Assay (CiPA) initiative – Update on progress. *J Pharmacol Toxicol Methods* **81**, 15–20.

Conti L, Renhorn J, Gabrielsson A, Turesson F, Liin SI, Lindahl E & Elinder F (2016). Reciprocal voltage sensor-to-pore coupling leads to potassium channel C-type inactivation. *Sci Rep* **6**, 27562.

Cordero-Morales JF, Cuello LG, Zhao Y, Jogini V, Cortes DM, Roux B & Perozo E (2006). Molecular determinants of gating at the potassium-channel selectivity filter. *Nat Struct Mol Biol* **13**, 311–318.

Cordomí A, Caltabiano G & Pardo L (2012). Membrane protein simulations using AMBER force field and Berger lipid parameters. *J Chem Theory Comput* **8**, 948–958.

Cornell WD, Cieplak P, Bayly CI, Gould IR, Merz KM, Ferguson DM, Spellmeyer DC, Fox T, Caldwell JW & Kollman PA (1995). A second generation force field for the simulation of proteins, nucleic acids, and organic molecules. *J Am Chem Soc* **117**, 5179–5197.

Corry B & Thomas M (2012). Mechanism of ion permeation and selectivity in a voltage gated sodium channel. *J Am Chem Soc* **134**, 1840–1846.

Cuello LG, Cortes DM & Perozo E (2017). The gating cycle of a K^+ channel at atomic resolution. *Elife* **6**, e28032.

Cuello LG, Jogini V, Cortes DM, Pan AC, Gagnon DG, Dalmas O, Cordero-Morales JF, Chakrapani S, Roux B & Perozo E (2010*a*). Structural basis for the coupling between activation and inactivation gates in K^+ channels. *Nature* **466**, 272–275.

Cuello LG, Jogini V, Cortes DM & Perozo E (2010*b*). Structural mechanism of C-type inactivation in K^+ channels. *Nature* **466**, 203–208.

Darve E, Rodríguez-Gómez D & Pohorille A (2008). Adaptive biasing force method for scalar and vector free energy calculations. *J Chem Phys* **128**, 144120.

Delemotte L (2018). Opening leads to closing: Allosteric crosstalk between the activation and inactivation gates in KcsA. *J Gen Physiol* **150**, 1356–1359.

Delemotte L, Kasimova MA, Klein ML, Tarek M & Carnevale V (2015). Free-energy landscape of ion-channel voltage-sensor-domain activation. *Proc Natl Acad Sci U S A* **112**, 124–129.

Delemotte L, Kasimova MA, Sigg D, Klein ML, Carnevale V & Tarek M (2017). Exploring the complex dynamics of an ion channel voltage sensor domain via computation. *bioRxiv*, https://doi.org/10.1101/108217.

DeMarco KR & Clancy CE (2016). Cardiac Na channels: structure to function. *Curr Top Membr* **78**, 287–311.

Deol SS, Domene C, Bond PJ & Sansom MS (2006). Anionic phospholipid interactions with the potassium channel KcsA: simulation studies. *Biophys J* **90**, 822–830.

Devaraneni PK, Komarov AG, Costantino CA, Devereaux JJ, Matulef K & Valiyaveetil FI (2013). Semisynthetic K^+ channels show that the constricted conformation of the selectivity filter is not the C-type inactivated state. *Proc Natl Acad Sci U S A* **110**, 15698–15703.

Dhakshnamoorthy B, Rohaim A, Rui H, Blachowicz L & Roux B (2016). Structural and functional characterization of a calcium-activated cation channel from *Tsukamurella paurometabola*. *Nat Commun* **7**, 12753.

Doyle DA, Morais Cabral J, Pfuetzner RA, Kuo A, Gulbis JM, Cohen SL, Chait BT & MacKinnon R (1998). The structure of the potassium channel: molecular basis of K^+ conduction and selectivity. *Science* **280**, 69–77.

Durdagi S, Deshpande S, Duff HJ & Noskov SY (2012). Modeling of open, closed, and open-inactivated states of the hERG1 channel: structural mechanisms of the state-dependent drug binding. *J Chem Inf Model* **52**, 2760–2774.

Durell SR, Shrivastava IH & Guy HR (2004). Models of the structure and voltage-gating mechanism of the Shaker K^+ channel. *Biophys J* **87**, 2116–2130.

Eastman P, Swails J, Chodera JD, McGibbon RT, Zhao Y, Beauchamp KA, Wang L-P, Simmonett AC, Harrigan MP & Stern CD (2017). OpenMM 7: Rapid development of high performance algorithms for molecular dynamics. *PLoS Comput Biol* **13**, e1005659.

Fernández-Mariño AI, Harpole TJ, Oelstrom K, Delemotte L & Chanda B (2018). Gating interaction maps reveal a noncanonical electromechanical coupling mode in the Shaker K^+ channel. *Nat Struct Mol Biol* **25**, 320.

Fiser A & Sali A (2003). Modeller: generation and refinement of homology-based protein structure models. *Methods Enzymol* **374**, 461–491.

Flood E, Boiteux C & Allen TW (2018). Selective ion permeation involves complexation with carboxylates and lysine in a model human sodium channel. *PLoS Comput Biol* **14**, e1006398.

Forrest LR, Tang CL & Honig B (2006). On the accuracy of homology modeling and sequence alignment methods applied to membrane proteins. *Biophys J* **91**, 508–517.

Fowler PW, Abad E, Beckstein O & Sansom MSP (2013). Energetics of multi-ion conduction pathways in potassium ion channels. *J Chem Theory Comput* **9**, 5176–5189.

Fowler PW & Sansom MS (2013). The pore of voltage-gated potassium ion channels is strained when closed. *Nat Commun* **4**, 1872.

Fukunishi H, Watanabe O & Takada S (2002). On the Hamiltonian replica exchange method for efficient sampling of biomolecular systems: Application to protein structure prediction. *J Chem Phys* **116**, 9058–9067.

Furini S & Domene C (2009). Atypical mechanism of conduction in potassium channels. *Proc Natl Acad Sci U S A* **106**, 16074–16077.

Gennis RB (1989). *Biomembranes: Molecular Structure and Function*. Springer-Verlag, New York.

Grizel AV, Glukhov GS & Sokolova OS (2014). Mechanisms of activation of voltage-gated potassium channels. *Acta Naturae* **6**, 10–26.

Gumbart J, Khalili-Araghi F, Sotomayor M & Roux B (2012). Constant electric field simulations of the membrane potential illustrated with simple systems. *Biochim Biophys Acta* **1818**, 294–302.

Harvey MJ & De Fabritiis G (2012). High-throughput molecular dynamics: the powerful new tool for drug discovery. *Drug Discov Today* **17**, 1059–1062.

Heer FT, Posson DJ, Wojtas-Niziurski W, Nimigean CM & Berneche S (2017). Mechanism of activation at the selectivity filter of the KcsA K^+ channel. *Elife* **6**, e25844.

Hess B, Bekker H, Berendsen HJ & Fraaije JG (1997). LINCS: a linear constraint solver for molecular simulations. *J Comput Chem* **18**, 1463–1472.

Hess B, Kutzner C, van der Spoel D & Lindahl E (2008). GROMACS 4: Algorithms for highly efficient, load-balanced, and scalable molecular simulation. *J Chem Theory Comput* **4**, 435–447.

Hille B (2001). *Ion Channels of Excitable Membranes*. Sinauer, Sunderland, MA, USA.

Hille B, Armstrong CM & MacKinnon R (1999). Ion channels: from idea to reality. *Nat Med* **5**, 1105–1109.

Hite RK & MacKinnon R (2017). Structural titration of Slo2.2, a Na^+-dependent K^+ channel. *Cell* **168**, 390–399. e311.

Hodgkin AL & Keynes RD (1955). The potassium permeability of a giant nerve fibre. *J Physiol* **128**, 61–88.

Horn HW, Swope WC, Pitera JW, Madura JD, Dick TJ, Hura GL & Head-Gordon T (2004). Development of an improved four-site water model for biomolecular simulations: TIP4P-Ew. *J Chem Phys* **120**, 9665–9678.

Hoshi T & Armstrong CM (2013). C-type inactivation of voltage-gated K^+ channels: pore constriction or dilation? *J Gen Physiol* **141**, 151–160.

Hoshi T, Zagotta WN & Aldrich RW (1991). Two types of inactivation in Shaker K^+ channels: effects of alterations in the carboxy-terminal region. *Neuron* **7**, 547–556.

Huang J & MacKerell AD Jr (2013). CHARMM36 all-atom additive protein force field: validation based on comparison to NMR data. *J Comput Chem* **34**, 2135–2145.

Huang J, Rauscher S, Nawrocki G, Ran T, Feig M, de Groot BL, Grubmuller H & MacKerell AD Jr (2017). CHARMM36m: an improved force field for folded and intrinsically disordered proteins. *Nat Methods* **14**, 71–73.

Im W, Seefeld S & Roux B (2000). A Grand Canonical Monte Carlo-Brownian dynamics algorithm for simulating ion channels. *Biophys J* **79**, 788–801.

Ing C & Pomes R (2016). Simulation studies of ion permeation and selectivity in voltage-gated sodium channels. *Curr Top Membr* **78**, 215–260.

Israelewitz B, Gao M & Schulten K (2001). Steered molecular dynamics and mechanical functions of proteins. *Curr Opin Struct Biol* **11**, 224–230.

Jacobson MP, Pincus DL, Rapp CS, Day TJF, Honig B, Shaw DE & Friesner RA (2004). A hierarchical approach to all-atom protein loop prediction. *Proteins* **55**, 351–367.

Jensen MO, Borhani DW, Lindorff-Larsen K, Maragakis P, Jogini V, Eastwood MP, Dror RO & Shaw DE (2010). Principles of conduction and hydrophobic gating in K^+ channels. *Proc Natl Acad Sci U S A* **107**, 5833–5838.

Jensen MO, Jogini V, Borhani DW, Leffler AE, Dror RO & Shaw DE (2012). Mechanism of voltage gating in potassium channels. *Science* **336**, 229–233.

Jensen MØ, Jogini V, Eastwood MP & Shaw DE (2013). Atomic-level simulation of current–voltage relationships in single-file ion channels. *J Gen Physiol* **141**, 619–632.

Jiang Y, Lee A, Chen J, Ruta V, Cadene M, Chait BT & MacKinnon R (2003). X-ray structure of a voltage-dependent K^+ channel. *Nature* **423**, 33–41.

Jorgensen WL, Chandrasekhar J, Madura JD, Impey RW & Klein ML (1983). Comparison of simple potential functions for simulating liquid water. *J Chem Phys* **79**, 926–935.

Joung IS & Cheatham III TE (2008). Determination of alkali and halide monovalent ion parameters for use in explicitly solvated biomolecular simulations. *J Phys Chem B* **112**, 9020–9041.

Kahlen J, Salimi L, Sulpizi M, Peter C & Donadio D (2014). Interaction of charged amino-acid side chains with ions: An optimization strategy for classical force fields. *J Phys Chem B* **118**, 3960–3972.

Kaminski GA, Friesner RA, Tirado-Rives J & Jorgensen WL (2001). Evaluation and reparametrization of the OPLS-AA force field for proteins via comparison with accurate quantum chemical calculations on peptides. *J Phys Chem B* **105**, 6474–6487.

Karpen ME, de Haseth PL & Neet KE (1992). Differences in the amino acid distributions of 3(10)-helices and alpha-helices. *Protein Science* **1**, 1333–1342.

Kasimova MA, Tarek M, Shaytan AK, Shaitan KV & Delemotte L (2014). Voltage-gated ion channel modulation by lipids: Insights from molecular dynamics simulations. *Biochim Biophys Acta* **1838**, 1322–1331.

Kass RS (2005). The channelopathies: novel insights into molecular and genetic mechanisms of human disease. *J Clin Invest* **115**, 1986–1989.

Khalili-Araghi F, Jogini V, Yarov-Yarovoy V, Tajkhorshid E, Roux B & Schulten K (2010). Calculation of the gating charge for the Kv1.2 voltage-activated potassium channel. *Biophys J* **98**, 2189–2198.

Kim I & Warshel A (2014). Coarse-grained simulations of the gating current in the voltage-activated Kv1.2 channel. *Proc Natl Acad Sci U S A* **111**, 2128–2133.

Koehler Leman J, Ulmschneider MB & Gray JJ (2015). Computational modeling of membrane proteins. *Proteins* **83**, 1–24.

Kollman P (1993). Free energy calculations: applications to chemical and biochemical phenomena. *Chem Rev* **93**, 2395–2417.

Kopec W, Köpfer DA, Vickery ON, Bondarenko AS, Jansen TL, de Groot BL & Zachariae U (2018). Direct knock-on of desolvated ions governs strict ion selectivity in K^+ channels. *Nat Chem* **10**, 813–820.

Köpfer DA, Song C, Gruene T, Sheldrick GM, Zachariae U & de Groot BL (2014). Ion permeation in K^+ channels occurs by direct Coulomb knock-on. *Science* **346**, 352–355.

Kratochvil HT, Carr JK, Matulef K, Annen AW, Li H, Maj M, Ostmeyer J, Serrano AL, Raghuraman H, Moran SD, Skinner JL, Perozo E, Roux B, Valiyaveetil FI & Zanni MT (2016). Instantaneous ion configurations in the K^+ ion channel selectivity filter revealed by 2D IR spectroscopy. *Science* **353**, 1040–1044.

Kutzner C, Grubmüller H, de Groot Bert L & Zachariae U (2011). Computational electrophysiology: the molecular dynamics of ion channel permeation and selectivity in atomistic detail. *Biophys J* **101**, 809–817.

Kutzner C, Köpfer DA, Machtens J-P, de Groot BL, Song C & Zachariae U (2016). Insights into the function of ion channels by computational electrophysiology simulations. *Biochim Biophys Acta* **1858**, 1741–1752.

Laio A & Parrinello M (2002). Escaping free-energy minima. *Proc Natl Acad Sci U S A* **99**, 12562–12566.

Lee S-Y, Lee A, Chen J & MacKinnon R (2005). Structure of the KvAP voltage-dependent K^+ channel and its dependence on the lipid membrane. *Proc Natl Acad Sci U S A* **102**, 15441–15446.

Lenaeus MJ, Gamal El-Din TM, Ing C, Ramanadane K, Pomès R, Zheng N & Catterall WA (2017). Structures of closed and open states of a voltage-gated sodium channel. *Proc Natl Acad Sci U S A* **114**, E3051-E3060.

Li H, Ngo V, Da Silva MC, Salahub DR, Callahan K, Roux B & Noskov SY (2015). Representation of ion-protein interactions using the Drude polarizable force-field. *J Phys Chem B* **119**, 9401–9416.

Li J, Ostmeyer J, Boulanger E, Rui H, Perozo E & Roux B (2017*a*). Chemical substitutions in the selectivity filter of potassium channels do not rule out constricted-like conformations for C-type inactivation. *Proc Natl Acad Sci U S A* **114**, 11145–11150.

Li J, Ostmeyer J, Cuello LG, Perozo E & Roux B (2018). Rapid constriction of the selectivity filter underlies C-type inactivation in the KcsA potassium channel. *J Gen Physiol* **150**, 1408–1420.

Li Q, Wanderling S, Paduch M, Medovoy D, Singharoy A, McGreevy R, Villalba-Galea CA, Hulse RE, Roux B, Schulten K, Kossiakoff A & Perozo E (2014). Structural mechanism of voltage-dependent gating in an isolated voltage-sensing domain. *Nat Struct Mol Biol* **21**, 244–252.

Li Y, Sun R, Liu H & Gong H (2017*b*). Molecular dynamics study of ion transport through an open model of voltage-gated sodium channel. *Biochim Biophys Acta* **1859**, 879–887.

Lindahl ER (2008). Molecular dynamics simulations. *Methods Mol Biol* **443**, 3–23.

Long SB, Campbell EB & Mackinnon R (2005*a*). Crystal structure of a mammalian voltage-dependent Shaker family K^+ channel. *Science* **309**, 897–903.

Long SB, Campbell EB & Mackinnon R (2005*b*). Voltage sensor of Kv1.2: structural basis of electromechanical coupling. *Science* **309**, 903–908.

Long SB, Tao X, Campbell EB & MacKinnon R (2007). Atomic structure of a voltage-dependent K^+ channel in a lipid membrane-like environment. *Nature* **450**, 376–382.

Lopes PE, Guvench O & MacKerell AD Jr (2015). Current status of protein force fields for molecular dynamics simulations. *Methods Mol Biol* **1215**, 47–71.

Luo Y & Roux B (2009). Simulation of osmotic pressure in concentrated aqueous salt solutions. *J Phys Chem Lett* **1**, 183–189.

Lyubartsev AP & Rabinovich AL (2016). Force field development for lipid membrane simulations. *Biochim Biophys Acta* **1858**, 2483–2497.

Mackerell AD Jr (2004). Empirical force fields for biological macromolecules: overview and issues. *J Comput Chem* **25**, 1584–1604.

Maffeo C, Bhattacharya S, Yoo J, Wells D & Aksimentiev A (2012). Modeling and simulation of ion channels. *Chem Rev* **112**, 6250–6284.

Mahdavi S & Kuyucak S (2015). Mechanism of ion permeation in mammalian voltage-gated sodium channels. *PLoS One* **10**, e0133000.

Marius P, Zagnoni M, Sandison ME, East JM, Morgan H & Lee AG (2008). Binding of anionic lipids to at least three nonannular sites on the potassium channel KcsA is required for channel opening. *Biophys J* **94**, 1689–1698.

Matthies D, Bae C, Toombes GE, Fox T, Bartesaghi A, Subramaniam S & Swartz KJ (2018). Single-particle cryo-EM structure of a voltage-activated potassium channel in lipid nanodiscs. *Elife* **7**, e37558.

Miyamoto S & Kollman PA (1992). SETTLE: an analytical version of the SHAKE and RATTLE algorithm for rigid water models. *J Comput Chem* **13**, 952–962.

Morais-Cabral JH, Zhou Y & MacKinnon R (2001). Energetic optimization of ion conduction rate by the K^+ selectivity filter. *Nature* **414**, 37–42.

Nishizawa M & Nishizawa K (2008). Molecular dynamics simulation of Kv channel voltage sensor helix in a lipid membrane with applied electric field. *Biophys J* **95**, 1729–1744.

Onufriev AV & Izadi S (2018). Water models for biomolecular simulations. *Wiley Interdiscip Rev Comput Mol Sci* **8**, e1347, https://doi.org/10.1002/wcms.1347.

Ostmeyer J, Chakrapani S, Pan AC, Perozo E & Roux B (2013). Recovery from slow inactivation in K^+ channels is controlled by water molecules. *Nature* **501**, 121–124.

Overington JP, Al-Lazikani B & Hopkins AL (2006). How many drug targets are there? *Nat Rev Drug Discov* **5**, 993–996.

Palamini M, Canciani A & Forneris F (2016). Identifying and visualizing macromolecular flexibility in structural biology. *Front Mol Biosci* **3**, 47.

Pan AC, Cuello LG, Perozo E & Roux B (2011). Thermodynamic coupling between activation and inactivation gating in potassium channels revealed by free energy molecular dynamics simulations. *J Gen Physiol* **138**, 571–580.

Pan X, Li Z, Zhou Q, Shen H, Wu K, Huang X, Chen J, Zhang J, Zhu X, Lei J, Xiong W, Gong H, Xiao B & Yan N (2018). Structure of the human voltage-gated sodium channel Nav1.4 in complex with β1. *Science* **362**, eaau2486.

Patel S, Davis JE & Bauer BA (2009). Exploring ion permeation energetics in gramicidin A using polarizable charge equilibration force fields. *J Am Chem Soc* **131**, 13890–13891.

Pathak MM, Yarov-Yarovoy V, Agarwal G, Roux B, Barth P, Kohout S, Tombola F & Isacoff EY (2007). Closing in on the resting state of the Shaker K^+ channel. *Neuron* **56**, 124–140.

Pau V, Zhou Y, Ramu Y, Xu Y & Lu Z (2017). Crystal structure of an inactivated mutant mammalian voltage-gated K^+ channel. *Nat Struct Mol Biol* **24**, 857–865.

Payandeh J, Gamal El-Din TM, Scheuer T, Zheng N & Catterall WA (2012). Crystal structure of a voltage-gated sodium channel in two potentially inactivated states. *Nature* **486**, 135–139.

Payandeh J, Scheuer T, Zheng N & Catterall WA (2011). The crystal structure of a voltage-gated sodium channel. *Nature* **475**, 353–358.

Peng X, Zhang Y, Chu H, Li Y, Zhang D, Cao L & Li G (2016). Accurate evaluation of ion conductivity of the gramicidin A channel using a polarizable force field without any corrections. *J Chem Theory Comput* **12**, 2973–2982.

Phillips JC, Braun R, Wang W, Gumbart J, Tajkhorshid E, Villa E, Chipot C, Skeel RD, Kale L & Schulten K (2005). Scalable molecular dynamics with NAMD. *J Comput Chem* **26**, 1781–1802.

Ponder JW (2004). TINKER: Software tools for molecular design. Washington University School of Medicine, Saint Louis, MO. https://dasher.wustl.edu/tinker.

Rasmusson RL, Morales MJ, Wang S, Liu S, Campbell DL, Brahmajothi MV & Strauss HC (1998). Inactivation of voltage-gated cardiac K^+ channels. *Circ Res* **82**, 739–750.

Rawson S, Davies S, Lippiat JD & Muench SP (2016). The changing landscape of membrane protein structural biology through developments in electron microscopy. *Mol Membr Biol* **33**, 12–22.

Rodriguez-Menchaca AA, Adney SK, Tang Q-Y, Meng X-Y, Rosenhouse-Dantsker A, Cui M & Logothetis DE (2012). PIP2 controls voltage-sensor movement and pore opening of Kv channels through the S4–S5 linker. *Proc Natl Acad Sci U S A* **109**, E2399–E2408.

Roux B (2017). Ion channels and ion selectivity. *Essays Biochem* **61**, 201–209.

Roux B, Allen T, Berneche S & Im W (2004). Theoretical and computational models of biological ion channels. *Q Rev Biophys* **37**, 15–103.

Rusinova R, Kim DM, Nimigean CM & Andersen OS (2014). Regulation of ion channel function by the host lipid bilayer examined by a stopped-flow spectrofluorometric assay. *Biophys J* **106**, 1070–1078.

Ryckaert J-P, Ciccotti G & Berendsen HJ (1977). Numerical integration of the cartesian equations of motion of a system with constraints: molecular dynamics of n-alkanes. *J Comput Phys* **23**, 327–341.

Schlitter J, Engels M & Krüger P (1994). Targeted molecular dynamics: a new approach for searching pathways of conformational transitions. *J Mol Graph* **12**, 84–89.

Schmid N, Eichenberger AP, Choutko A, Riniker S, Winger M, Mark AE & van Gunsteren WF (2011). Definition and testing of the GROMOS force-field versions 54A7 and 54B7. *Eur Biophys J* **40**, 843.

Schmidt D, Jiang Q-X & MacKinnon R (2006). Phospholipids and the origin of cationic gating charges in voltage sensors. *Nature* **444**, 775.

Schwaiger CS, Bjelkmar P, Hess B & Lindahl E (2011). 3_{10}-Helix conformation facilitates the transition of a voltage sensor S4 segment toward the down state. *Biophys J* **100**, 1446–1454.

Seoh SA, Sigg D, Papazian DM & Bezanilla F (1996). Voltage-sensing residues in the S2 and S4 segments of the Shaker K^+ channel. *Neuron* **16**, 1159–1167.

Shaw DE, Grossman JP, Bank JA, Batson B, Butts JA, Chao JC, Deneroff MM, Dror RO, Even A, Fenton CH, Forte A, Gagliardo J, Gill G, Greskamp B, Ho CR, Ierardi DJ, Iserovich L, Kuskin JS, Larson RH, Layman T, Lee LS, Lerer AK, Li C, Killebrew D, Mackenzie KM, Mok SYH, Moraes MA, Mueller R, Nociolo LJ, Peticolas JL, Quan T, Ramot D, Salmon JK, Scarpazza DP, Ben Schafer U, Siddique N, Snyder CW, Spengler J, Tang PTP, Theobald M, Toma H, Towles B, Vitale B, Wang SC & Young C (2014). Anton 2: Raising the bar for performance and programmability in a special-purpose molecular dynamics supercomputer. Sc14: International Conference for High Performance Computing, Networking, Storage and Analysis, 41–53.

Sheldrick GM (2015). Crystal structure refinement with SHELXL. *Acta Crystallogr C Struct Chem* **71**, 3–8.

Shen H, Zhou Q, Pan X, Li Z, Wu J & Yan N (2017). Structure of a eukaryotic voltage-gated sodium channel at near-atomic resolution. *Science* **355**, eaal4326.

Silva JR, Pan H, Wu D, Nekouzadeh A, Decker KF, Cui J, Baker NA, Sept D & Rudy Y (2009). A multiscale model linking ion-channel molecular dynamics and electrostatics to the cardiac action potential. *Proc Natl Acad Sci U S A* **106**, 11102–11106.

Song YF, DiMaio F, Wang RYR, Kim D, Miles C, Brunette TJ, Thompson J & Baker D (2013). High-resolution comparative modeling with RosettaCM. *Structure* **21**, 1735–1742.

Southan C, Sharman JL, Benson HE, Faccenda E, Pawson AJ, Alexander SP, Buneman OP, Davenport AP, McGrath JC, Peters JA, Spedding M, Catterall WA, Fabbro D, Davies JA & NC-UPHAR (2016). The IUPHAR/BPS Guide to PHARMACOLOGY in 2016: towards curated quantitative interactions between 1300 protein targets and 6000 ligands. *Nucleic Acids Res* **44**, D1054–D1068.

Starek G, Freites JA, Berneche S & Tobias DJ (2017). Gating energetics of a voltage-dependent K^+ channel pore domain. *J Comput Chem* **38**, 1472–1478.

Sugita Y & Okamoto Y (1999). Replica-exchange molecular dynamics method for protein folding. *Chem Phys Lett* **314**, 141–151.

Sula A, Booker J, Ng LCT, Naylor CE, DeCaen PG & Wallace BA (2017). The complete structure of an activated open sodium channel. *Nat Commun* **8**, 14205.

Sun RN & Gong H (2017). Simulating the activation of voltage sensing domain for a voltage-gated sodium channel using polarizable force field. *J Phys Chem Lett* **8**, 901–908.

Tao X, Lee A, Limapichat W, Dougherty DA & MacKinnon R (2010). A gating charge transfer center in voltage sensors. *Science* **328**, 67–73.

Tao X & MacKinnon R (2008). Functional analysis of Kv1.2 and paddle chimera Kv channels in planar lipid bilayers. *J Mol Biol* **382**, 24–33.

Tobias DJ & Brooks CL 3rd (1991). Thermodynamics and mechanism of alpha helix initiation in alanine and valine peptides. *Biochemistry* **30**, 6059–6070.

Toombes GE & Swartz KJ (2016). Twists and turns in gating ion channels with voltage. *Science* **353**, 646–647.

Torrie GM & Valleau JP (1977). Nonphysical sampling distributions in Monte Carlo free-energy estimation: Umbrella sampling. *J Comput Phys* **23**, 187–199.

Treptow W, Marrink SJ & Tarek M (2008). Gating motions in voltage-gated potassium channels revealed by coarse-grained molecular dynamics simulations. *J Phys Chem B* **112**, 3277–3282.

Tuckerman M, Berne BJ & Martyna GJ (1992). Reversible multiple time scale molecular dynamics. *J Chem Phys* **97**, 1990–2001.

Ubarretxena-Belandia I & Stokes DL (2010). Present and future of membrane protein structure determination by electron crystallography. *Adv Protein Chem Struct Biol* **81**, 33.

Ulmschneider MB, Bagnéris C, McCusker EC, DeCaen PG, Delling M, Clapham DE, Ulmschneider JP & Wallace BA (2013). Molecular dynamics of ion transport through the open conformation of a bacterial voltage-gated sodium channel. *Proc Natl Acad Sci U S A* **110**, 6364–6369.

Valiyaveetil FI, Zhou Y & MacKinnon R (2002). Lipids in the structure, folding, and function of the KcsA K^+ channel. *Biochemistry* **41**, 10771–10777.

Vandenberg JI, Perozo E & Allen TW (2017). Towards a structural view of drug binding to hERG K^+ channels. *Trends Pharmacol Sci* **38**, 899–907.

Vandenberg JI, Perry MD, Perrin MJ, Mann SA, Ke Y & Hill AP (2012). hERG K^+ channels: structure, function, and clinical significance. *Physiol Rev* **92**, 1393–1478.

Vargas E, Yarov-Yarovoy V, Khalili-Araghi F, Catterall WA, Klein ML, Tarek M, Lindahl E, Schulten K, Perozo E, Bezanilla F & Roux B (2012). An emerging consensus on voltage-dependent gating from computational modeling and molecular dynamics simulations. *J Gen Physiol* **140**, 587–594.

Venable RM, Luo Y, Gawrisch K, Roux B & Pastor RW (2013). Simulations of anionic lipid membranes: development of interaction-specific ion parameters and validation using NMR data. *J Phys Chem B* **117**, 10183–10192.

Vorobyov I, Bekker B & Allen TW (2010). Electrostatics of deformable lipid membranes. *Biophys J* **98**, 2904–2913.

Vorobyov I, Li L & Allen TW (2008). Assessing atomistic and coarse-grained force fields for protein-lipid interactions: the formidable challenge of an ionizable side chain in a membrane. *J Phys Chem B* **112**, 9588–9602.

Wang W & MacKinnon R (2017). Cryo-EM structure of the open human *ether-à-go-go*-related K^+ channel hERG. *Cell* **169**, 422–430.e10.

Whicher JR & MacKinnon R (2016). Structure of the voltage-gated K^+ channel Eag1 reveals an alternative voltage sensing mechanism. *Science* **353**, 664–669.

Xu Y, Bhate MP & McDermott AE (2017). Transmembrane allosteric energetics characterization for strong coupling between proton and potassium ion binding in the KcsA channel. *Proc Natl Acad Sci U S A* **114**, 8788–8793.

Yan Z, Zhou Q, Wang L, Wu J, Zhao Y, Huang G, Peng W, Shen H, Lei J & Yan N (2017). Structure of the Nav1.4-β1 complex from electric eel. *Cell* **170**, 470–482.e411.

Yarov-Yarovoy V, Allen TW & Clancy CE (2014). Computational models for predictive cardiac ion channel pharmacology. *Drug Discov Today Dis Models* **14**, 3–10.

Yarov-Yarovoy V, DeCaen PG, Westenbroek RE, Pan CY, Scheuer T, Baker D & Catterall WA (2012). Structural basis for gating charge movement in the voltage sensor of a sodium channel. *Proc Natl Acad Sci U S A* **109**, E93–E102.

Yazdi S, Stein M, Elinder F, Andersson M & Lindahl E (2016). The molecular basis of polyunsaturated fatty acid interactions with the *Shaker* voltage-gated potassium channel. *PLoS Comput Biol* **12**, e1004704.

Yu H, Mazzanti CL, Whitfield TW, Koeppe RE, Andersen OS & Roux B (2010). A combined experimental and theoretical study of ion solvation in liquid *N*-methylacetamide. *J Am Chem Soc* **132**, 10847–10856.

Zagotta WN, Hoshi T & Aldrich RW (1990). Restoration of inactivation in mutants of Shaker potassium channels by a peptide derived from ShB. *Science* **250**, 568–571.

Zhang J, Mao W, Ren Y, Sun R-N, Yan N & Gong H (2018). Simulating the ion permeation and ion selection for a eukaryotic voltage-gated sodium channel NaVPaS. *Protein Cell* **9**, 580–585.

Zhang X, Ren W, DeCaen P, Yan C, Tao X, Tang L, Wang J, Hasegawa K, Kumasaka T, He J, Wang J, Clapham DE & Yan N (2012). Crystal structure of an orthologue of the NaChBac voltage-gated sodium channel. *Nature* **486**, 130–134.

Zhou Y & MacKinnon R (2003). The occupancy of ions in the K^+ selectivity filter: charge balance and coupling of ion binding to a protein conformational change underlie high conduction rates. *J Mol Biol* **333**, 965–975.

Zhou Y, Morais-Cabral JH, Kaufman A & MacKinnon R (2001). Chemistry of ion coordination and hydration revealed by a K^+ channel-Fab complex at 2.0 Å resolution. *Nature* **414**, 43–48.

Zhu X, Lopes PE & MacKerell AD (2012). Recent developments and applications of the CHARMM force fields. *Wiley Interdiscip Rev Comput Mol Sci* **2**, 167–185.

Zimmermann L, Stephens A, Nam SZ, Rau D, Kubler J, Lozajic M, Gabler F, Soding J, Lupas AN & Alva V (2018). A completely reimplemented MPI bioinformatics toolkit with a new HHpred server at its core. *J Mol Biol* **430**, 2237–2243.

Zwier MC & Chong LT (2010). Reaching biological timescales with all-atom molecular dynamics simulations. *Curr Opin Pharmacol* **10**, 745–752.

Additional information

Competing interests

None declared.

Author contributions

K.R.D., S.B. and I.V. performed literature search, drafted and revised the manuscript and devised the figures. K.R.D. illustrated the figures. I.V. coordinated the project and prepared the manuscript. All authors have read and approved the final version of this manuscript and agree to be accountable for all aspects of the work in ensuring that questions related to the accuracy or integrity of any part of the work are appropriately investigated and resolved. All persons designated as authors qualify for authorship, and all those who qualify for authorship are listed.

Funding

K.R.D. is supported by the American Heart Association Pre-doctoral Fellowship (16PRE27260295), Western States Affiliate. K.R.D., S.B. and I.V. are supported by the National Institutes of Health NHLBI grants 5U01HL126273 and 5R01HL128537. K.R.D. and I.V. are also supported by the National Institutes of Health grant 1OT2OD026580.

Acknowledgements

We would like to thank Prof. Colleen E. Clancy and Jon T. Sack for their help in manuscript preparation as well as helpful discussions along with Profs Vladimir Yarov-Yarovoy and Heike Wulff.